Response to Editor

Main concerns 1)
inclusion and propagation of uncertainties

We have expanded the discussion on measurement uncertainties as follows:

"The typical 5-min measurement precision is 0.3 ‰ for δ^{13}C and 0.05 µmol mol^{-1} for CO_2 mole fraction according to the instrument manufacturer. Our own Allan variance analysis revealed a precision of 0.05 ‰ for δ^{13}C and 0.07 ppm for CO_2 mole fraction at the hourly averaging interval. The precision of the ambient measurement was lower than this due to error propagated through the calibration procedure. According to a laboratory test on an analyzer of the same model and using the same calibration procedure as ours, the hourly δ^{13}C precision is about 0.4 ‰ (Wen et al., 2013). The calibration gases have much lower δ^{13}C than the ambient delta values. The mismatch in the delta value between the calibration standard and the ambient air is common in applications of the IRIS technique (^{13}C in methane, Röckmann et al. 2016; ^{18}O in water vapor, Lee et al. 2005; ^{13}C in CO_2, Bowling et al. 2003). But because the system measures the concentrations of the major and the minor isotopologue independently, it is not critical that the calibration standard and the measurement target have matching isotope ratios (Bowling et al. 2005)."

Main concerns 2)
regression via Miller-Tans and Keeling methods

Thank you for your recommendations on the papers relevant to this topic. After careful reading of these papers, we now realize that the geometric mean regression method we used originally is not a good choice. We now use the ordinary least squares regression. This point is noted in the Methods section:

"For the purpose of comparing with the Miller-Tans results, we also estimated the source isotope ratio using the Keeling mixing line method. According to Wehr and Saleska (2017), at the measurement uncertainties of our instrument system, the ordinary least squares procedure has much lower bias errors of parameter estimation than the geometric mean regression. In the following, the results of both the Miller-Tans method and the Keeling mixing line method were based on the ordinary least squares regression."

The change in the regression method caused the mean δ_S to decrease by an average amount of 0.9 ‰. As a result, the partitioned biological flux in the YRD changed from being a weak sink to a weak source.

Main concerns 3)
Please include uncertainties in all source isotope delta end members (delta_F, delta_C, delta_P) and fluxes (F_F and F_C) propagate errors formally, stating the values and uncertainties of each term. A Monte Carlo analysis is not justified because the underlying mass-balance equations are explicit. Disregarding the fact that it is not needed for the propagation of errors, the MC analysis (in l. 459-467) omits the uncertainties in the fluxes F_F and F_C and the isotope deltas delta_S and delta_C. Most importantly, the uncertainty treatment should not be dealt with "as an afterthought", but should be carried out consistently throughout the mnauscript.

We have now included uncertainties in all isotope delta end members and the fluxes (Tables 2 and 3; Figures 6 - 8).

The Monte Carlo procedure is used frequently by the hydrological community to quantify uncertainties associated with the partitioning of hydrological inputs to lake systems from isotope end members. There, the partitioning equations are also explicit expressions of the mass conservation principle. We used the same procedure to quantify how uncertainties in the isotope end members and the anthropogenic fluxes propagate through the partitioning equations. (In this updated analysis, we have considered uncertainties in all the input terms. Thank you for your suggestion.)

We now treat the issue of uncertainty throughout the paper. We have added the following description to the Methods section:

"The partitioning equations are explicit expression of the mass balance principle. But uncertainties in the isotope delta end members and the anthropogenic fluxes can propagate through these equations, causing uncertainties in the estimation of F_S and F_P. Here we used a Monte Carlo analysis to quantify these uncertainties. The same analysis has been applied to the partitioning of lake water budgets from isotope end members (Jasechko et al. 2014). The procedure employed a Gaussian distribution for errors in the input variables and an ensemble of 10,000 realizations for each month. Errors in F_S and F_P were computed as one standard deviation of these realizations after excluding the top and bottom 50 extreme ensemble members."

Main concerns 4)
The fact that your Miller-Tans regressions (Fig. 3 and Fig. 4) show non-zero intercepts provides the insight that they are not a suitable method to analyse the data on the annual timescale. You need to provide evidence that the method is suitable on shorter time-scales, in particular, the monthly timescale you are envisaging. A suitable timescale would be one that results in a non-zero intercept. You might find that a monthly timescale is not appropriate either, in which case an even more finely-grained analyses would be required, e.g. diel or even hourly, with subsequent aggregation of the derived source isotope deltas into daily/monthly/annual means. This was already pointed out by Referee #1. Please include a set of figures (Miller-Tans plots) that shows the data aggregated to subannual time-scales (monthly, possibly diel) and state the resulting source isotope deltas and their uncertainties.

That the Miller-Tans intercept is not zero is indeed a cause of concern. At the monthly time scale, the original Miller-Tans method has a non-zero intercept in the range of 300 to 900 ‰ μmol mol^{-1}. (A monthly example is now provided in Supplementary Figure S2.)

Following your suggestion, we have tried the 5-hour moving-window technique described by Vardag et al. (2016) for January and July 2014. Only 4 % of the data (all obtained at nighttime) satisfies their data screening criteria. The mean regression equation is $y = -26.41$ (± 4.03) $x + 428.84$ ($\pm$ 211.12) for January and $y = -25.64$ (± 6.39) $x + 687.83$ ($\pm$ 264.67) for July, where x is (C_a-C_b) and y is $\delta_a C_a$.

That the intercept does not go to zero even at such a short-time scale leads us to hypothesize that the concentration and isotope measurements at the WMO baseline background site

(WLG) do not represent the true background for this highly urbanized region. We have also applied the method to other isotope data published for urban areas, and found that the problem seems common for urban studies. Most of these urban datasets yield nonzero intercepts (Supplementary Figure S3 and Table S1).

In the end, we decided to replace the WLG measurement with the tropospheric CO_2 concentration calculated by CarbonTracker over the YRD region as the background. To overcome the problem that CarbonTracker does not calculate tropospheric $\delta^{13}C$, we rearranged the original Miller-Tans equation to a form that allows an intercept but without the need for a known background $\delta^{13}C$. The changes of the background and the regression equation cause δ_S to decrease slightly by a mean value of 0.1 ‰, in comparison to the results obtained with the WLG as the background and the original Miller-Tans equation.

Please refer to Section 2.2 (which is completely rewritten) for additional explanation.

Main concerns 5)
I've tried to replicate the slope of -12 ‰ (instead of -24 ‰), which Referee #2 reported in their review posted on 3 October 2016, but have not been able to.

Thank you for checking on this. A surface source isotope ratio of -12 ‰ would seem too high to us.

Detailed Comments:
(1) l. 33: Why do you restrict "daytime" to 1000-1600 and "nighttime" to 2200-0600, omitting the hours in between?

We have added the following explanation:
"Morning and evening transitional periods were omitted to avoid the confounding effects of sign change of the biological flux and sudden changes in the atmospheric stability regime."

(2)l. 162: Please describe how the standard gases were calibrated against NBS 19 (no hyphen) and NBS 20 (with space) and report the individual results of these measurements before conversion to the VPDB scale. What δ(13C) values (w.r.t. VPDB) did you use for NBS 20? The standard gases are a long way removed from the atmospheric value and virtually identical. This introduced significant scale uncertainties, see paper by Coplen et al. New guidelines for 13C measurements. Anal. Chem. 78, 2439-2441.

We apologize for a mixed-up here. NBS 19 and NBS 20 were used in an earlier study (Wen et al. 2013). In the present study, the reference materials were actually IAEA-CO-8 and IAEA-CO-9. We have added these details:

"… their δ13C values were measured with a mass spectrometer (MAT-253, Finnigan) using IAEA reference materials IAEA-CO-8 (-5.76 ‰ VPDB) and IAEA-CO-9 (-47.32 ‰ VPDB). The mass spectrometer measurements of these reference materials were (-5.81 ± 0.04) ‰ and (-46.64 ± 0.08) ‰ before normalization to the VPDB scale."

Please refer to our response to Main point 1 regarding the mismatch between the calbiration gas isotope ratio and the ambient isotope ratio.

(3)l. 169: What do you mean by removing "40 3-minute data points"? Data over 3-minute intervals on 40 different occasions? Did this apply to all calibration gas runs? Were there only 40 calibration gas runs in the whole dataset? Perhaps your response could include a schematic or figure to illustrate what you have done.

This sentence has been changed to:
"We removed the first 3 min of the data after switching to the ambient sampling mode from the calibration mode."

(4)l. 170: Why were these data removed?

We remove the first 2-min data because the analyzer needed time to adjust to the step change after valve switching (Supplementary Figure S1).

(5)l. 204: Where were the Mount Waliguan data obtained? Please give a reference to the data depository and state how the data were measured, by whom and which instrument was used.

An online reference is added

(6)The 2015 WLG data are now available, so the analysis should be performed with the actual data rather than some extrapolated version.

We have updated this analysis using the actual observations at WLG.

(7)What efforts have been made to ensure that the new data are compatible (i.e. on the same scale) as the WLG data. What is the uncertainty of the delta(13C) of the a) WLG data and b) the new data with respect to VPDB?

The measurements at WLG are traceable to standards supplied by NOAA-ERL. The CO_2 concentration of our calibration gases was calibrated against three primary standards (with known mole fraction but unknown $\delta^{13}C$) obtained from NOAA-ERL. One of us (Wen) has recently acquired $\delta^{13}C$ gas standards from NOAA-ERL, but unfortunately our working standards had already been depleted by then.

We have added the following text to the Methods section:
"Table 1 lists the concentrations and their isotopic compositions of the standard gases used in this study. These gases were balanced in air. Their CO2 mole fractions were measured with an IRIS analyzer (model G1101-i, Picarro Inc.) and calibrated against three primary standards obtained from NOAA-ERL which were traceable to the WMO 2007 scale reported by the Central Calibration Laboratory of the World Meteorological Organization, and their δ13C values were measured with a mass spectrometer (MAT-253, Finnigan) using IAEA reference materials IAEA-CO-8 (-5.76 ‰ VPDB) and IAEA-CO-9 (-47.32 ‰ VPDB)."

Technical corrections:
(1)There should always be a space between value and unit, incl. per cent and per mill symbols, e.g. "-8.48 ‰", "13 %", "15 ºC". There is no space before the degree sign if it refers to a geographic coordinate, but there is a space before the compass direction: "33º N". Please correct these errors throughout the manuscript.

Changed throughout the whole paper.

(2)Please use SI units for mole fractions, i.e. "µmol mol-1", not ppm, which is ambiguous.

Changed.

(3)Units and chemical symbols must not be mixed. The name of the quantity should identify the species of interest, i.e. "the CO2 mass flux", and the unit should simply be "mg m-2 s-1" (e.g. l. 254).

Corrected

(4)Please note that in line with international conventions, indices should be enclosed in brackets after the quantity symbol, including δ values, i.e. the correct notation is "δ(13C)". Unfortunately, in the past, the isotope geochemistry community has ignored this convention, but this is not a good reason to continue this poor practice. Alternatively, you might want to omit the index and just write "δ" because - at least in the context of the present manuscript - only 13C/12C isotope ratios are considered. This makes also for a more concise terminology when you discuss the isotope delta of sources (Eq. 5), which would then be "δ_S" instead of "δ_S(13C)", see comment on line 97 below. As you are not qualifying the mole fraction symbol further in Eq. 1, I suggest you should omit the index "(13C)" entirely.

We now use the symbols you recommended, such as δ_S, δ_F, δ_C, and δ_a.

(5)The language used at a number of places in the manuscript is not as clear as it should be. Please make the following changes to rectify this. Terms like "13C isotope composition", "13C isotopic signature", "highly enriched 13C signal", etc. do not make sense because they must be quantified by reference to the other stable carbon isotope, 12C.

Corrected.

(6)l. 24: This is grammatically wrong. Please change to "Observations of mole fraction and carbon stable isotope composition (expressed as δ(13C)) of CO2 in urban ...".

Corrected

(7)l. 25: Add "and sinks" after sources.

Added.

(8)l. 26: Replace "C" with "carbon". Please make the same change everywhere else in the manuscript as well. Unncessary abbreviations should be avoided for clarity and easier reading.

Replaced.

(9)l. 29 & 30: Please also give the standard deviations of mean mole fraction and delta(13C).

Done.

(10)l. 31: Change word order to "highly 13C-enriched". Delete "the" before "Mount Waliguan".

Corrected.

(11)l. 34: Change to "we showed that the δ(13C) of CO2 sources"

Changed

(12)l. 43: Change to "unique 13C/12C ratios" or "unique δ(13C) values" or "unique carbon stable isotope signatures".

Changed.

(13)l. 48: Replace "isotopic signature" with "δ(13C)".

Replaced

(14)l. 49: Replace "heavier" with "higher".

Replaced.

(15)l. 51: Replace "13C composition" with "δ(13C)".

Replaced

(16)l. 55: Replace "δ13C" with "carbon stable isotope".

Replaced

(17)l. 56: "13C signature" - see l. 43.

Replaced

(18)l. 74, 87, 96, 123, 145: Delete "its" (mole fractions don't have δ(13C) values).

Deleted

(19)l. 97 & elsewhere: Wrong order of indices - this should be δ_S(13C).

Corrected

(20)l. 114: Either add the index "(13C)" to the delta symbols on the left hand side of the equation or omit it from the right hand side.

Changed.

(21)l. 115: "at a background site"

Edited

(22)l. 116: Please rephrase. Mole fractions don't have isotopic compositions, and there is no such thing as a "13C isotopic composition", also see comments above.

Changed to “mole fraction and δ^{13}C value of CO_2” throughout the paper.

(23)l. 125: "built-up area"

Edited.

(24)l. 127: Change to "190 million" and add a space before the compass direction (e.g. "33.41° N").

Edited

(25)Replace hyphens with to, e.g. "29.04° to 33.41° N".

Replaced

(26)l. 129: Rephrase to "The main vegetation types are all C3 species".

Rephrased

(27)l. 150: I find it hard to believe that there was no other anthropogenic CO2 source within a 3 km radius. Are there no houses? No heating system? No humans? No cars?

This sentence has been changed to “There was no large industrial CO_2 source in the 3 km radius…”

(28)l. 152: Please delete the "~" (tilde) sign and give an accurate distance instead (rounded and/or with uncertainties, if necessary). In any case, the "~" sign is not the correct symbol to designate approximations (for which "≈" should be used).

Corrected

(29)l. 162: Please describe

Please refer to detailed comments 2 and 7.

(30)l. 173: Do you mean "high bias" or "high error"? And if bias, do you mean "biased high" (i.e. too large) or "highly biased" (i.e. biased a lot, but unclear in which direction)? How much is the bias (or error)?

Changed to “is biased high”

(31)l. 181: Do you mean relative humidity? In any case, the symbol "V" before "%" must be omitted.
Use SI units, i.e. 0.66 cmol/mol, or 0.66 x 10^(-2) m^3/m^3, for mole fractions (or volume fractions).

Edited. This is now referred to as “water vapor mole fraction”

(32)l. 181: Please replace "13C composition" with "13C/12C ratio".

Edited

(33)l. 185: Which one is it? A volume fraction? Or a mole fraction? Do you make a correction for the non-ideality of the gases involved?

It is mole fraction. We did not correct for non-ideality.

(34)l. 188: This equation is wrong (or at least inconsistent with the text). The second term on the right hand side should most likely be 0.46 ‰ (H/% - 2.03).

Edited

(35)l. 189: Please delete "in percent". Physical quantities are not limited to one specific unit.

Deleted

(36)l. 190: Please change "isotopic composition" to "isotope delta" (two occurrences).

Changed

(37)l. 193: has -> have

Changed

(38)l. 253: Replace 13C isotope composition with an adequate term - see comments above.

Replaced as“δ^{13}C value”

(39)l. 255: Units and chemical symbols should not be mixed. If you want to specify the species the fluxes refer to, it should be enclosed in brackets, e.g. F_s(CO2), or you could explain in the text that "F" relates to CO2 mass fluxes. The unit should be written as "mg m-2 s-1".

Changed.

(40)l. 258: "unknowns to be solved for"

Edited

(41)l. 264: adapt -> adopt

Edited

(42)l. 264: State the value used for delta(13C) of CO2 released during cement production, and its uncertainty. The uncertainty should be propagated through the flux calculation.

Done.

(43)l. 264: You should calculate an uncertainty for delta_P and propagate it to your flux calculation.

Done.

(44)l. 271: What is the uncertainty of this value?

The 20 % value is based on an eddy covariance observation. The nighttime F_F is also assumed to have an uncertainty of 10 %.

(45)l. 288-290: What are the standard deviations of these values?

Information added.

(46)l. 292: Replace "diurnal" with "diel". Diurnal means "during the day"; "diel" means "over 24 hours".

Replaced.

(47)l. 293: Define the winter season - which months?

Defined (December to February).

(48)l. 301: Value and uncertainty must be enclosed in brackets so that the unit symbol applies to both, i.e. (-24.75±0.26) ‰. Please revise this and similar occurrences throughout the manuscript.

All checked

(49)l. 301: bound -> limit

Edited

(50)l. 307-321: This whole section is missing uncertainties and their propagation through the calculation.

Uncertainty ranges are now provided.

(51)l. 316: The delta differences have been calculated incorrectly. These should be 1.53 ‰ and 0.53 ‰ because the delta scale is not linear.

This comparison has been removed. (We have replaced Figures 4 and 5 with plots of the data obtained in January 2014.)

(52)l. 319: What do you mean by "linear correlation"? Is that the slope? Please give the full result of the regression (slope and intercept) including uncertainties of slope and intercept and

state the R^2 value.

These are linear correlation coefficients. The detailed regression statistics are now added.

(53)Section 3.3: Again uncertainty estimates are missing as well as their propagation.

The uncertainty ranges are now included in Tables 2 and 3.

(54)l. 349, 449, etc.: There should be a space between "m-2" and "s-1".

Changed.

(55)l. 369: "consistent"

Edited.

(56)l. 379: What do you by "varied 70% to 80% in winter and about 50% in summer"? In the remainder of the paragraph you use fractional comparison between winter and summer.

Changed to "In Chicago, natural gas usage comprises 70 % to 80 % of total fossil fuel consumption in the winter and about 50 % in the summer (Moore and Jacobson 2015)"

(57)l. 421/2: "monthly mean" (x 2)

Edited.

(58)l. 422: "WLG value"

Edited.

(59)l. 459-467: This MC analysis omits the uncertainties in the fluxes F_F and F_C and the isotope deltas delta_S and delta_C and should be improved by including them.

This analysis has been updated with the uncertainties in FF and Fc. The uncertainties in the partitioned fluxes are now shown (Figures 7 and 8).

(60)l. 493: The correlation coefficient is not a meaningful figure of merit to compare the "goodness of fit" by a Keeling plot regression and by a Miller-Tans regression because they plot different variables on the axes. It would be more useful to state the resulting uncertainties of the source delta values, delta_S(13C).

We have deleted this portion of the text. Thank you.

(61)l. 853: "diel variation"

Edited

(62)Figure 1: x-axis label should be x(H2O)/% or y(H2O)/%.

We kept the original x-axis label but changed the independent variable in Equation 2 to “H_2O” to be consistent with this data plot.

(63)Figure 5: x-axis label.

Edited

(64)Figs. 7 & 8: The lack of variability in F_F seems to be implausible. What variability would you expect? Please indicate this on the plot and include it in the uncertainty propagation.

All the variables are now given an uncertainty range.

Response to Referee 2

This paper uses continuous measurements of the stable isotopic composition of carbon (δ13C) in CO2 to investigate CO2 emissions in the city of Nanjing and the surrounding areas, taking advantage of differing footprints for night (Nanjing) and day (surrounding area) times of day. The most important observation is that some of the δ^{13}C values are higher than background. The only mechanism to produce this is by incorporating emissions from cement production, which is characterized by very high δ^{13}C values of +0.20 ‰.

Main concerns 1)
The major concern in this paper is that the authors are using the Miller-Tans (2003) approach to determine the average monthly δ13C of the sources for daytime and nighttime. In that formulation, the background values of CO2 mole fractions and δ13C are included in the linear equation, with the slope being the δ13C of the highCO2 endmember. The equation for this analysis is:
δobsCobs - δbgCbg = δs(Cobs - Cbg)
where δobsCobs - δbgCbg is plotted against (Cobs - Cbg). There should be no intercept determined during the analysis. However, the plots shown in Figures 4 and 5 show significant non-zero intercepts. I have looked at the data from the supplement, together with the NOAA data from WLG, which is being used as background in this new version, and found that the intercepts for the nighttime data for 2013-2014 should be ~-12‰ with a zero intercept, instead of -24 ‰ as shown in Figure 5. My analysis was approximate, in that I used a smoothing spline for interpolating the WLG data, instead of the Thoning et al. (1989) smoothing code. However, these are very different values and should affect the fluxes being calculated. At minimum, the meaning of the intercept values should be discussed, as well as why it is calculated.

Please refer to our response to the editor

Specific comments:
(1)Line 35 and often throughout: Give uncertainties or standard deviations of ranges.

Added

(2)Line 120: After "(Miller et al. 2003)" add "and was used in an urban environment by Newman et al. (2016)."

Added

(3)Line 121: Insert "continuous measurements in" between "to" and "an urban environment."

Added

(4)Line 138: You have justified using the Miller-Tans method earlier in the Introduction. There is no reason to discuss the performance of the Keeling plot method. Also, you do not show any Keeling plots. This discussion is left over from the previous version of the manuscript.

We now include the Keeling plot results (Figure 6; Supplementary Table S2).

(5)Lines 160–162: The carbon isotopic compositions of the two standards (Table 1) are very similar and very far from the values of the ambient measurements. Can you show that there are no extrapolation uncertainties?

Please refer to our response to the editor.

(6)Lines 287–289: What does it mean to say that δ13C values display a larger seasonal cycle than do CO2 mole fraction values? The latter is ~20 ppm, whereas the former ~2‰. Are you thinking about a relative fraction?

This sentence is changed to "The $^{13}C/^{12}C$ ratio of atmospheric CO_2 displayed a more clear seasonal cycle than the mole fraction."

(7)Lines 299–321: The Miller-Tans (2003) method assumes a zero intercept. What is the meaning of your intercept, and how does it affect the interpretation of the slope?

Please refer to our response to the editor.

(8)Lines 311 –321: What is the significance of these observations? Are they important enough that you should show figure(s) with the correlations?

We have added this sentence:
"These correlation patterns suggest that atmospheric $\delta^{13}C$ was influenced more by surface sources at the regional scale than at the local (city) scale."

(9)Lines 348–355: A lot of values are given – what are the uncertainties?

The uncertainties of these values are now given.

(10)Lines 369–370: Replace with: "to 2013, which was consistent with the seasonal variation of background and transport of emissions from fossil fuel combustion (Newman et al. 2016)."

Replaced

(11)Line 418: "Park Falls"

Edited

(12)Line 420: "fossil fuel combustion which has low 13C contents." This depends on the nature of the fossil fuel component. As shown in Table 2, gasoline combustion produces CO2 with δ13C very similar to the biosphere, and combustion of coal produces CO2 with values higher than the biosphere.

This sentence has been changed to "…the plant photosynthetic enhancement of ^{13}C is offset by the CO_2 from fossil fuel combustion which has lower $^{13}C/^{12}C$ ratios than the atmosphere."

(13)Lines 477–504: Remove this section. It is left over from the previous version and no longer necessary

We now present the Keeling results.

Response to Referee 3

The authors made an obvious effort to improve the paper, and addressed most of my concerns reasonably well. There are still some weak points, and I realize that the work needed to fix some of them may be not possible anymore. I list my last concerns below and I leave it to the editor to decide if any of them is important enough to delay the publication.

Main concerns 1)
The accuracy is still not addressed in the answer or in the paper (but I do realize that this may be difficult with the information available). The precision for 1-hr intervals is specified; however, the calibration is done using 2-min averaged data, which will have lower precision; in this case the dataset could show 3-hourly steps due to the calibration.

Please refer to our response to the editor.

Main concerns 2)
The final NOAA data for 2015 for WLG are available. Did the authors at least check whether their extrapolated data for 2015 are somewhat similar to the real data from NOAA? (this should be easy)

Done. Thank you.

Main concerns 3)
the two sets of calibration gases listed in Table 1 have identical isotope values – please check if this is correct

This is because the two sets came from the same mixtures of CO_2 and air.

Main concerns 4)
I still find the estimation of uncertainties of the main results poor, and also the answers to the reviewers questions related to this. When comparing average mole fractions or isotope values (for examples Nanjing with WLG), the uncertainty should be given, in order to decide if the values are significantly different or not. For the final flux results, the Monte Carlo simulation estimates the influence of a 1‰ error in δ13Cp and δ13Cf, but does not account for the other variables that contribute to the overall uncertainty (Ff, Fc, δ13Cs, δ13Cc). Also, the results are only discussed in text as overall averages; when looking at Figs 7 and 8, it is not clear without errors shown which of the values are different from zero and if any of the variability is significant.

Please refer to our response to the editor.

Interpreting the $^{13}C/^{12}C$ ratio of carbon dioxide in an urban airshed in the Yangtze River Delta, China

Jiaping Xu[1], Xuhui Lee[1,2*], Wei Xiao[1], Chang Cao[1], Shoudong Liu[1], Xuefa Wen[3], Jingzheng Xu[1], Zhen Zhang[1], Jiayu Zhao[1]

[1]Yale-NUIST Center on Atmospheric Environment, Nanjing University of Information Science & Technology, Nanjing, China

[2]School of Forestry and Environmental Studies, Yale University, New Haven, Connecticut, USA

[3]Key Laboratory of Ecosystem Network Observation and Modeling, Institute of Geographic Sciences and Natural Resources Research, Chinese Academy of Sciences, Beijing, China

* Corresponding author
Dr. Xuhui Lee
Sara Shallenberger Brown Professor
School of Forestry and Environmental Studies, Yale University,
21 Sachem Street, New Haven, Connecticut 06510, USA
Phone: (203)432-6271; Fax: (203)432-5023
E-mail: xuhui.lee@yale.edu

Abstract: Observations of atmospheric CO_2 mole fraction and the~~its~~ $^{13}C/^{12}C$ ~~isotope~~ ratio~~composition~~ (expressed as $\delta^{13}C$) in urban airsheds provide constraints on the roles of anthropogenic and natural sources and sinks in local and regional carbon~~C~~ cycles. In this study, we report observations of these quantities in Nanjing at hourly intervals from March 2013 to August 2015 using a laser-based optical instrument. Nanjing is the second largest city located in the highly industrialized Yangtze River Delta (YRD), Eastern China. The mean CO_2 mole fraction and $\delta^{13}C$ were (439.7 ± 7.5) µmol mol^{-1} and (-8.48 ± 0.56) ‰ ~~439.7 ppm and -8.48‰~~ over this observational period. The peak monthly mean $\delta^{13}C$ (-7.44 ‰, July 2013) was 0.74 ‰ higher than that observed at ~~the~~ Mount Waliguan, a WMO baseline site on the Tibetan Plateau and upwind of the YRD region. The highly ~~enriched~~ ^{13}C-enriched signal was partly attributed to the influence of cement production in the region. By applying the Miller-Tans method to nighttime and daytime observations to represent signals from the city of Nanjing and the YRD, respectively, we showed that the~~-~~ $^{13}C/^{12}C$ ratio ~~^{13}C signal~~ of CO_2~~C~~ sources in the Nanjing Municipality was (0.21 ± 0.53)~~48~~ ‰ lower than that in the YRD. Flux partitioning calculations revealed that natural ecosystems in the YRD were a negligibly small source~~sink~~ of atmospheric CO_2~~, consistent with the Carbon Tracker inverse modeling result~~.

Formatted: Superscript

Formatted: Superscript

Formatted: Subscript

Keywords: urban areas; CO_2 flux; Industrial process; Carbon isotope; In-situ observation

1 Introduction

Atmospheric CO_2 sources and sinks in urban areas consist mainly of plant uptake and release and fossil fuel combustion. These contributors have unique ^{13}C/^{12}C ratios~~isotopic signatures~~. City clusters are human-dominated systems with high carbon emission intensity, contributing over 70% of the total anthropogenic CO_2 to the atmosphere (Satterthwaite 2008). Previous urban isotopic studies emphasize carbon emissions from fossil combustion (Zondervan and Meijer 1996, Pataki et al. 2003, Zimnoch et al. 2004, Affek and Eiler 2006, Newman et al. 2008). Relatively little attention is given to the δ^{13}C~~isotopic signature~~ of carbon dioxide released by cement production, which is much high~~heavi~~er than that of fossil fuel origin (Andres et al. 1994). Likewise, the CO_2 emitted from burning of minerals in non-energy consumption industrial processes, such as iron and steel production, has higher δ^{13}C ~~^{13}C composition~~ than that of fossil fuel (Table 2~~1~~, Widory 2006). In China, cement production and industrial processes contribute 13 % of the total anthropogenic CO_2 emission (Mu et al. 2013). Many of these industrial activities occur in or near urban areas. So far, little is known about their roles in the atmospheric ~~δ^{13}C~~ carbon stable isotope budget.

Formatted: Superscript

One scientific motivation for quantifying the ~~^{1}~~δ^{13}C~~^{3}C signature~~ of atmospheric CO_2 is that it provides constraints that allow partitioning of the net surface flux into component fluxes (Farquhar and Lloyd 1993, Yakir and Sternberg 2000, Pataki et al. 2003). The ^{13}C-based partitioning method has been used primarily for vegetation ecosystems, such as forests (Lloyd et al. 1996, Lloyd et al. 2001, Ometto, et al. 2006, Zobitz et al. 2008), grasses (Ometto et al. 2002, Pataki et al. 2003), and crops (Leavitt et al. 1995, Griffis et al. 2005). The approach has also been used in a limited number of urban studies (Pataki et al. 2003, Zimnoch et al. 2004, Newman et al. 2008, Jasek et al. 2014). Compared with vegetation ecosystems, urban ecosystems have more complex CO_2 source configuration. We must consider both natural sources (plants and soils) and anthropogenic sources (fossil combustion and non-energy industrial processes) and the fact that the degree of mixing of urban air with the free troposphere and the air outside the urban boundary varies diurnally and seasonally. Anthropogenic emissions are hard to quantify because they depend on multiple factors including city size, population density, fossil mix, and climate.

One of the first measurements of the carbon isotope ratio~~composition~~ of CO_2 in an urban atmosphere was made by Friedman and Irsa (1967). Since then, a few more experiments have been conducted in urban environments. The data collected have been used to partition CO_2 contributors (Koerner and Klopatek 2002, Clark-Thorne and Yapp 2003), to quantify die~~urna~~l variations in the CO_2 mole fraction and ~~its~~ $\delta^{13}C$ in urban air (Zimnoch et al. 2004, Guha and Ghosh 2010) and across urban to rural gradients (Lichtfouse et al. 2003, Pataki et al. 2007), and variations among different land uses in urban areas (Clark-Thorne and Yapp 2003, Widory and Javoy 2003). The isotopic data reveal insights into energy consumption patterns (Widory and Javoy 2003, Bush et al. 2007), impacts of meteorology including temperature (Clark-Thorne and Yapp 2003, Zimnoch et al. 2004), atmospheric stability (Pataki et al. 2005) and wind (Clark-Thorne and Yapp 2003) on urban carbon cycling, and the role of vegetation phenology (Ehleringer et al. 2002, Takahashi et al. 2002, Wang and Pataki 2012). The analytical technique employed in these studies is mainly based on mass-spectrometry (MS). Because sample collection, preparation and analysis are labor intensive, the majority of these studies are limited to short campaigns (less than 60 days).

In recent years, the development of isotope ratio infrared spectroscopy (IRIS) and on-line calibration technology provides a new solution for long-term in-situ observation of the CO_2 mole fraction and ~~its~~ δ^{13}C at high frequencies (1 Hz to 1 hour; Pataki et al. 2006, Griffis. 2013, Gorski et al. 2015). Compared with the MS method, IRIS can capture die~~urna~~l or even shorter temporal variations with relatively high accuracy, enabling us to understand how anthropogenic emissions change atmopheric CO_2 at highly resolved temporal and spatial scales. Nevertheless, application of the IRIS technology in urban monitoring is still limited in terms of cities covered and measurement duration: less than 35 days in McManus et al. (2002), Pataki et al. 2006 and Wada et al. (2011) and 3 seasons in Moore and Jacobson (2015). Only a few~~one~~ published studies~~y~~ have~~s~~ presented data that span~~s~~ one full annual cycle (Pang et al. 2016; Vardag et al. 2016).

Simultaneous measurement of atmospheric CO_2 concentration and~~–~~ δ^{13}C ~~its isotopic composition~~ is used to determine the overall ^{13}C/^{12}C~~isotopic~~ ratio~~signature~~ of local surface sources δ~~^{13}C~~$_{\mathrm{S}}$. The majority of~~All~~ published urban studies to date have deployed the Keeling plot method (Keeling 1958, Keeling 1961) for the determination of δ~~^{13}C~~$_{\mathrm{S}}$. In this approach, a linear relationship is established between δ^{13}C and the reciprocal of the CO_2 mole fraction from the observed time series, and the intercept of the linear regression is taken as the isotopic ratio~~composition~~ of the local CO_2 emissions. The method assumes that the isotopic ratio~~signature~~ of the sources is invariant with time. It also assumes that changes in the CO_2 mole fraction and in δ^{13}C are attributed only to the surface sources and are unaffected by regional carbon sources (Pataki et al. 2003). However, these assumptions do not strictly hold in an urban environment because the intensity of traffic emissions varies strongly through the

Formatted: Superscript

Formatted: Superscript

die~~urna~~l cycle (McDonald et al. 2014), and therefore the composition~~composition~~ of the surface source varies, and its $^{13}C/^{12}C$ ratio~~signature~~ cannot be assumed constant. In addition, because of strong atmospheric mixing in the daytime convective boundary layer, the background air in the upper troposphere can be easily entrained to the surface layer, mixing the CO_2 that originates from regional sources with that emitted locally in the urban airshed.

Miller and Tans (2003) propose that δ~~^{13}C~~$_S$ be determined as the slope of the linear relationship

$\delta_a C_a - \delta_b C_b = \delta_S (C_a - C_b)$ ~~$\delta_a C_a - \delta_b C_b = \delta^{13} C_s (C_a - C_b)$~~

(1)

where C_a is CO_2 mole fraction in urban air, C_b is CO_2 mole fraction at~~in~~ a background site, δ_a is the ~~^{13}C~~ $\delta^{13}C$ ~~isotopic composition~~value ~~–~~of C_a, and δ_b is the ~~–^{13}C~~ $\delta^{13}C$ value ~~isotopic composition~~ of C_b. B~~We argue that b~~ecause this approach takes into account the fact the background atmosphere varies, it may be~~is~~ more suitable than the Keeling method for inferring δ~~^{13}C~~$_S$ from the observations made in the urban area with complex emission sources. The method has been applied to local and regional carbon budget studies in nonurban settings (Miller et al. 2003) and in an urban environment by Newman et al. (2016)~~.~~. Here we extend the method to continuous measurements in an urban environment.

In this study, we report the results of long-term (30 months) continuous measurement of atmospheric CO_2 mole fraction and ~~its~~ $\delta^{13}C$ at a suburban site in Nanjing using an IRIS instrument. Nanjing is the second largest city in the Yangtze River Delta (YRD), Eastern China, with a built~~d~~-up area of 753 km^2 and a population of 8.2 million. Geographically, the YRD includes the provinces of Jiangsu, Zhejiang and Anhui and the Shanghai municipality

Formatted: Superscript

Formatted: Font: (Default) Times New Roman, 12 pt

Formatted: Superscript

(29.04° to ~~-~~33.41° N, 118.33° to ~~-~~122.95° E) with a population of 1~~.~~90~~ hundred~~ million. The YRD is influenced by subtropical moist monsoon climate. The mean annual temperature is about 15 °C and the annual precipitation is between 1000 mm and 1800 mm. The ~~main~~ vegetation types~~, all of which~~ are all C3 species. The YRD is the most industrialized region in China and had a higher urban land fraction of 10.8 % as of 2014 than the global mean (2.4 %, Akbari et al. 2009). In 2014, more than 220 large cement production factories (daily output exceeding 1000 tons) were located in the YRD (China Cement, 2016), contributing about 20 % of the national cement output.

The objectives of this study are (1) to characterize the atmospheric δ^{13}C die~~urna~~l, seasonal and annual variations in this urban environment, in a region where such measurement is nonexistent, (2) to investigate the influence of cement production on atmospheric δ^{13}C, (3) to evaluate the performance of the Keeling plot and the Miller-Tans method for determining δ~~^{13}C~~$_{S}$, and (4) to explore the utility of the isotopic constraints for inferring the net surface flux and the plant CO_2 flux in Nanjing and in the YRD.

2 Methods

2.1 Atmospheric observation

An IRIS analyzer (model G1101-i, Picarro Inc., Sunnyvale, CA) was used to measure atmospheric CO_2 mole fraction and~~ its~~ ^{13}C/^{12}C ~~isotope~~ ratio~~composition~~ (δ^{13}C) continuously from February 2013 to August 2015. The analyzer was housed on the 9th floor of our laboratory building on the campus of Nanjing University of Information, Science and Technology (NUIST, 32°12' N, 118°43' E), in the northern suburb of Nanjing, at a linear

Formatted: Superscript

distance of 20 km to the city center. The instrument inlet was at a height of 34 m above the ground. There was no large industrial~~anthropogenic~~ CO_2 source in the 3 km radius except for a commuting road located about 300 m east of the observation site. The nearest industrial complex, the Nanjing Iron & Steel Group Co. Ltd. and the Nanjing Chemical Industry Group, was located about ~~∼~~5 km to the south of the site.

The measurement was made at 0.3 Hz and at an air flow rate of 30 mL min^{-1} at standard temperature and pressure. One three-way solenoid valve was combined with two two-way solenoid valves, so the analyzer could be switched for atmospheric sampling and for sampling of two standard gases. Calibration was carried out every 3 h by sampling each standard gas for 5 minutes following the procedure of Bowling et al. (2003) and Wen et al. (2013). (To avoid transient effects, only the data collected in the last 2 minutes of the 5-min calibration periods –was used; Supplementary Figure S1.~~.~~) Table 1 lists the concentrations and their isotopic ratio~~composition~~s of the standard gases used in this study. These gases were balanced in air. Their –CO_2 mole fractions were measured with a gas analyzer (model (model G1301, Picarro) and calibrated against three primary standards obtained from NOAA-ERL which were~~of the standard gases was traceable~~ traceable to the WMO 2007 scale reported by the Central Calibration Laboratory of the World Meteorological Organization, and their $\delta^{13}C$ values were measured with a mass spectrometer (MAT-253, Finnigan) using~~was based on the~~ IAEA reference materials IAEA-CO-8 (-5.76 ‰ VPDB) and IAEA-CO-9 (-~~NBS 19~~47.32 ‰ VPDB)~~ and the NBS20 standards of NIST~~. The mass spectrometer measurements of these reference materials were (-5.81 ± 0.04) ‰ and (-46.64 ± 0.08) ‰ before normalization to the VPDB scale~~-~~. The ambient measurement was averaged to hourly

Formatted: Indent: First line: 0.29" intervals. The isotopic ratio ~~composition~~ was expressed in the delta notation (δ^{13}C) in reference to the VPDB scale.

The typical 5-min measurement precision is 0.3 ‰ for δ^{13}C and 0.05 µmol mol^{-1}~~ppm~~ for CO$_2$ mole fraction according to the instrument manufacturer. Our own Allan variance analysis revealed a precision of 0.05 ‰ for δ^{13}C and 0.07 µmol mol^{-1}~~ppm~~ for CO$_2$ mole fraction at the hourly averaging interval. The precision of the ambient measurement was lower than this due to errors propagated through the calibration procedure. According to a laboratory test on an analyzer of the same model and using the same calibration procedure as ours, the hourly δ^{13}C precision is about 0.4 ‰ (Wen et al., 2013). The calibration gases had much lower δ^{13}C than the ambient delta values. The mismatch in the delta value between the calibration standard and the ambient air is common in applications of the IRIS technique [^{13}C(CH$_4$), Röckmann et al. 2016; ^{18}O(H$_2$O), Lee et al. 2005; ^{13}C(CO$_2$), Bowling et al. 2003]. But because the system measures the concentrations of the major and the minor isotopologue independently, it is not critical that the calibration standard and the measurement target have matching isotope ratios (Bowling et al. 2005).

Formatted: Font: Symbol

Formatted: Superscript

Formatted: Superscript

Formatted: Subscript

Formatted: Superscript

Formatted: Subscript

Formatted: Superscript

Formatted: Subscript

We did not adopt the strict filtering technique used for background sites (Thoning et al. 1989) because of high natural variations in urban airsheds. We removed the first 3 min of the data ~~40 3-minute data points during the transient periods~~ after switching to the ambient sampling mode from the calibration mode~~ion gas changes~~. Additionally, data were removed if hourly CO$_2$ mole fraction was lower than 390 µmol mol^{-1}~~ppm~~ or δ^{13}C were out of the range between -15 ‰ and -5.5 ‰.

The δ^{13}C value measured by the analyzer in high humidity conditions is~~suffers a high~~ biased high ~~error~~ due to spectral broadening and direct spectral interference (Rella 2011)~~.~~. To correct for the humidity interference, we carried out two tests using a dew-point generator (model 610, LI-COR, Inc., Lincoln, NE). A CO_2 standard gas (secondary standard gas, 439 µmol mol^{-1}~~ppm~~ in test one and 488 µmol mol^{-1}~~ppm~~ in test two, balanced by dry air) was fed into the dew-point generator. The outlet of the dew-point generator was connected with a 3-way union with one end linked to the inlet of the analyzer and the other open to the room. The humidity level of the air coming out of the dew point generator was regulated at eight levels in a dew-point temperature range of 1 to~~and~~ 30 °C, giving a water vapor mole fraction~~humidity~~ ranging from 0.66 ~~V~~% to 4.26 ~~V~~% (0.66 to 4.26 cmol mol^{-1}). Because the ^{13}C/^{12}C ratio~~^{13}C composition~~ of the standard gas was constant, any observed variations were caused by the humidity artifact. We found that no correction was needed for our analyzer if the water vapor mole fraction~~humidity~~ was below 2.03 %. Above this humidity level, the measurement was biased high by 0.46 ‰ for every 1 cmol mol^{-1}~~%~~ increase in the water vapor ~~vapor volume or~~ mole fraction (Figure 1). The two tests, taken eight months apart, yielded essentially the same result. The correction equation is

$$\delta^{13}C = \delta^{13}C_{true} \qquad H_2O \leq 2.03\ \% \qquad (2a)$$

$$\delta^{13}C = \delta^{13}C_{true} + 0.46\ ‰\ (H_2O\ \% - 2.03) \qquad H_2O > 2.03\ \% \qquad (2b)$$

~~$\delta^{13}C = \delta^{13}C_{true} \qquad H \leq 2.03\% \qquad (2a)$~~

~~$\delta^{13}C = \delta^{13}C_{true} + 0.46(H - 2.03) \qquad H > 2.03\% \qquad (2b)$~~

where H_2O is water vapor ~~volume~~ mole fraction~~ in percent,~~, ~~–~~δ^{13}C is the measured isotope delta~~ic composition~~ value (after the two-point calibration), and $\delta^{13}C_{true}$ is the true isotope

Formatted: Superscript

Formatted: Superscript

Formatted: Superscript

Formatted: Font: Symbol

Formatted: Superscript

Formatted: Font: Symbol

Formatted: Superscript

Formatted: Subscript

Formatted: Subscript

Formatted: Font: Symbol

Formatted: Superscript

Formatted: Font: Symbol

Formatted: Superscript

Formatted: Subscript

Formatted: Subscript

Formatted: Subscript

Formatted: Subscript

delta value~~ic composition~~. The ambient vapor mole fraction ~~humidity~~ varied from 0.16 to 3.64 ~~V~~% during the measurement period. About 35 % of the observations exceeded the threshold mole fraction~~humidity~~ of 2.03 %~~V~~ and required correction. The largest hourly correction was 0.74 ‰. In the following, all the data have~~s~~ been corrected for the humidity interference.~~–~~

2.2 The ^{13}C/^{12}C ~~isotop~~ratio~~ic composition~~ ~~($\delta^{13}C_S$)~~ of surface sources (δ_S)

We applied the Miller-Tans method to estimate the ^{13}C/^{12}C ratio of the surface source (δ_S). Strictly, Equation 1 does not allow a non-zero intercept, but when applied to the data obtained at the monthly time scale, the regression yielded a non-zero intercept (Supplementary Figure S2). To determine if a shorter time scale would improve the result, we applied the 5-h moving window technique described by Vardag et al. (2016) to the observations made in January and July 2014. Only 4 % of the data, all obtained at nighttime, satisfies their data screening criteria. The mean regression equation of this subset is y = (-26.41 ±4.03) x + (428.84 ± 211.12) for January and y = (-25.64 ±6.39) x + (687.83 ± 264.67) for July, where x is (C_a - C_b) and y is ($\delta_a C_a$ - $\delta_b C_b$). In these analyses, the background CO_2 mole fraction and the isotope ratio~~the data collected in daytime hours (10:00 to 16:00 local time; Equation 1) to represent YRD and to the data collected during nighttime hours (22:00-6:00 local time) to represent Nanjing. The slope was obtained by linear regression of (C_a-C_b) against ($\delta_a C_a$-$\delta_b C_b$) over monthly intervals. The monthly mean CO_2 mole fraction and the isotopic composition of the~~ ~~background air~~ were those observed at Mount Waliguan (WLG, 36°17' N, 100°54' E, 3816 m above the mean sea level; ~~Zhou et al.,~~

Formatted: Superscript

Formatted: Superscript

Formatted: Superscript

Formatted: Superscript

Formatted: Font: Not Bold

Formatted: Subscript

Formatted: Subscript

Formatted: Subscript

~~2005~~https://www.esrl.noaa.gov/gmd/dv/data/index.php) located at the northeastern edge of the Tibetan Plateau (Zhou et al., 2005), the closest upwind WMO background station for Nanjing.~~–~~ Use of other WMO baseline sites as the background gave essentially the same results. ~~Because the WLG data were not available for 2015 at the time of this analysis, we fitted the WLG data of both CO_2 and $\delta^{13}C$ with a four-harmonic quadratic function (Thoning et al. 1989) using the dataset from 2000 to 2014, and then used the function to estimate the monthly $\delta^{13}C_b$ and C_b values for 2015.~~

The selection of a background site is a critical issue when applying the Miller-Tans method (Ballantyne et al., 2011 & 2010~~, Turnbull et al., 2015~~). That the Miller-Tans intercept does not go to zero suggests that the baseline site WLG may not be a suitable background for this highly urbanized region. We tested the Miller-Tans method with other isotope data published for urban areas, and found that the intercept was nonzero for most of the urban datasets (Supplementary Figure S3 and Table S1).

In the following, we used the tropospheric CO_2 mole ratio calculated by CarbonTracker over the YRD region (altitude 3330 m; https://www.esrl.noaa.gov/gmd/dv/data/index.php) as the background concentration (C_b). The CarbonTracker mole ratio is on average 3.5 μmol mol^{-1} higher than that observed at WLG. To overcome the problem that CarbonTracker does not calculate tropospheric $\delta^{13}C$, we rearranged Equation 1 to a form that allows an intercept but without the need for a known background $\delta^{13}C$, as

$$\delta_a C_a = \delta_S (C_a - C_b) + \delta_b C_b \qquad (3)$$

The $^{13}C/^{12}C$ ratio of the surface source was taken as the slope of the linear regression of $\delta_a C_a$ against (C_a - C_b). A key difference between Equation 3 here and Equation 5 of Miller and Tans

Formatted: Subscript

Formatted: Subscript

Formatted: Font: Symbol

Formatted: Superscript

Formatted: Indent: First line: 0 ch

Formatted: Superscript

Formatted: Superscript

(2003) is that the δ_S appears only in the slope parameter in Equation 3 but in both the slope and the intercept parameter in Miller and Tans' Equation 5.

The Miller-Tans analysis was performed over monthly intervals, using ~~Ideally, the background site should not be affected by local and regional emission and should lie in the upwind direction of the observation site. Based on these criteria, we chose WLG as the background site for our analysis.~~ the data collected in daytime hours (10:00 to 16:00 local time~~; Equation 1~~) to represent YRD and~~ to the~~ data collected during nighttime hours (22:00-6:00 local time) to represent Nanjing. Morning and evening transitional periods were omitted to avoid the confounding effects of sign change of the biological CO_2 flux and sudden changes in the atmospheric stability regime. ~~The slope was obtained by linear regression of (Ca-Cb) against (δaCa-δbCb) over monthly intervals. The monthly mean CO2 mole fraction and the isotopic composition of the~~

Formatted: Subscript

We interpreted the daytime results to represent the influence of surface sources in the YRD region and the nighttime results to represent the influence of surface sources in the Nanjing municipality. The vigorous turbulent exchange in the daytime boundary layer diminishes the role of local sources in the measured concentration and isotopic ratio. In other words, the daytime measurement has a much larger source footprint than the size of the urban land itself or the footprint of the nighttime measurement. In contrast, the buildup of CO_2 at night is primarily the result of sources in the city (Shen et al. 2014), so we considered the δ~~^{13}C~~$_S$ determined from the nighttime observations to represent the signal of the sources located in the city. Admittedly, this interpretation of daytime versus nighttime source areas is a simplification because the actual source area also depends on thermal stratification and boundary layer wind. Nevertheless, it is supported by a trajectory analysis and by an analysis of the atmospheric methane to CO_2 emissions ratio (Shen et al. 2014).

For the purpose of comparing with the Miller-Tans results, we also estimated the source ^{13}C/^{12}C ratio using the Keeling mixing line method. According to Wehr and Saleska (2017), at the measurement uncertainties of our instrument system, the ordinary least squares procedure has much lower bias errors of parameter estimation than the geometric mean regression. In the following, the results of both the Miller-Tans method and the Keeling mixing line method were based on the ordinary least squares regression.

Formatted: Superscript

Formatted: Superscript

2.3 Inventory of anthropogenic sources

We calculated the anthropogenic CO_2 fluxes from energy consumption and industrial process following the SCOPE 1 procedure issued by the International Council for Local Environmental Initiatives (ICLEI, 2008). The procedure considers only emissions from sources that lie within the geographic boundary of investigation. The energy consumption source consists of direct emissions from the three main energy consumption sectors (industry, transport, and household). We ignored the commerce sector here because the main energy consumption in this sector in Nanjing and in the YRD was electric power generated by coal and coal consumption which was already considered in SCOPE 1. The amounts of CO_2 emission were estimated with the IPCC methodology adopting the emission factors for each fossil fuel type recommended by IPCC. The calculations were done separately for the YRD region and for the Nanjing municipality. Because no statistical data were available for energy consumption in the transport sector in Nanjing, the CO_2 emission from the transport sector was deduced according to vehicle number, average annual driving distance and coefficients of fuel economy (Bi et al. 2011). We obtained the data on energy consumption from official sources (CESY 2013, CSY 2013, NSY, 2013).

The non-energy industrial processes included cement, raw iron, crude steel, and ammonia synthesis processes. In the YRD, the data were available at monthly intervals. For the city of Nanjing, only annual statistics were available.

2.4 Partitioning the net surface flux

We partitioned the surface CO$_2$ flux (F$_S$) into three component fluxes according to the following mass conservation equations

$$F_S=F_F+F_C+F_P$$

(4)

$$\delta_S F_S = \delta_F F_F + \delta_C F_C+\delta_P F_P$$

(~~$\delta^{13}C_SF_S=\delta^{13}C_FF_F+\delta^{13}C_CF_C+\delta^{13}C_PF_P$~~

~~(~~5)

where F$_F$ is the flux from fossil fuel combustion and industrial emission except cement production (termed “fossil plus”), F$_C$ is the flux due to cement production, F$_P$ is the biological flux, and δ~~^{13}C~~$_F$, δ~~^{13}C~~$_C$, and δ~~^{13}C~~$_{P}$~~$_P$~~ are the δ^{13}C value~~^{13}C isotope composition~~ of F$_F$, F$_C$ and F$_P$, respectively. These CO$_2$ mass fluxes are obtained by dividing the total emission by the surface area within the geographic boundary of Nanjing or the YRD, having dimensions of mg~~ CO$_2$~~ m^{-2} s^{-1}. We separated the cement source from other non-energy consumption industrial processes because its ^{13}C/^{12}C~~isotopic~~ ratio i~~signature i~~s much higher. In these

Formatted: Indent: First line: 0.29"

Formatted: Font: Symbol

Formatted: Subscript

Formatted: Font: Symbol

Formatted: Subscript

Formatted: Subscript

Formatted: Font: Symbol

Formatted: Subscript

Formatted: Subscript

Formatted: Font: Symbol

Formatted: Subscript

Formatted: Subscript

Formatted: Font: Symbol

Formatted: Superscript

Formatted: Subscript

Formatted: Subscript

Formatted: Superscript

Formatted: Superscript

equations, the monthly net surface flux (F_S) and the biological flux (F_P) are unknowns to be solved for, and all other terms are either provided by the atmospheric measurement or by the inventory calculation. The partitioning analysis was done for both Nanjing and the YRD using the nighttime and daytime observations, respectively.

The δ~~^{13}C~~$_F$ was weighted average of the isotope ratio~~δ^{13}C signal~~ of individual fuel types and industrial processes (~~Widory 2006;~~ Table 2). The~~ isotop~~ delta value~~ic composition~~ of CO_2 from cement production is provided by~~ Tans (1981) and~~ Anders (1994). We ado~~a~~pt a value of (-28.2 ‰) for δ~~^{13}C~~$_P$ for the YRD and Nanjing, on account of a linear relationship between δ~~^{13}C~~$_P$ and tree age (Fessenden and Ehleringer 2002), a typical tree age in this region (40 years) and an U-shaped relationship between δ~~^{13}C~~$_P$ and annual precipitation (Pataki et al. 2007). Our δ~~^{13}C~~$_P$ is more negative than that reported for a boreal forest (-26.2 ‰; Pataki et al. 2007) but is in closer agreement with the value reported for a Ginkgo tree in Nanjing (-29.3 ‰; Sun et al. 2003). A summary of the isotopic ratio~~composition~~s of the three source categories is given in Table 3.

Uncertainties in the delta values of the different fuel types and industrial processes were based on the data found in the references listed in Table 2. The uncertainty in δ_P was assumed to be ± 1.00 ‰ (Verdag et al. 2016). The mass flux terms F_F and F_C were assumed to have a 10% uncertainty, which is typical of fossil fuel consumption data (Vardag et al. 2016).

To partition the nighttime flux for Nanjing, we assumed that the nighttime F_F was 20 % of the daily value. The parameter 20 % was determined by the die~~urna~~l variation of the CO_2 flux observed with an eddy covariance system in Nanjing (Bai 2011) and in several other cities (Coutts et al. 2007, Song and Wang. 2011, Liu et al. 2012). At night, most of the

Formatted: Font: 12 pt

factories in the city were closed and the traffic flow was reduced to about 80 % of the daytime volume (Yang et al. 2011).

The partitioning equations are explicit expression of the mass balance principle. But uncertainties in the isotope delta end members and the anthropogenic fluxes can propagate through these equations, causing uncertainties in the estimation of F_S and F_P. Here we used a Monte Carlo analysis to quantify the error propagation. The same analysis has been applied to the partitioning of lake water budgets from isotope end members (Jasechko et al. 2014). The procedure employed a Gaussian distribution for errors in the input variables and an ensemble of 10,000 realizations for each month. Errors in F_S and F_P were computed as one standard deviation of these realizations after excluding the top and bottom 50 extreme ensemble members.

Formatted: Font: Not Italic

3. Results

3.1. Temporal variations in the CO_2 mole fraction and $\delta^{13}C$

The monthly CO_2 mole fraction during the summer was slightly lower than in the other seasons (Figure 2). The mean mole fraction was 446.7 µmol mol^{-1}~~ppm~~ and 431.1 µmol mol^{-1}~~ppm~~ for January and July, respectively, giving a seasonal amplitude of 15.6 µmol mol^{-1}~~ppm~~. The mean CO_2 mole fraction was 439.7 µmol mol^{-1}~~ppm~~ during the whole experimental period (March 2013 to August 2015), which is 40.6 µmol mol^{-1} ~~ppm~~ higher than the value observed ~~and estimated~~ at WLG for the same period. In 2014, the calendar year with complete data coverage, the mean CO_2 mole fraction was 441.2 µmol mol^{-1}~~ppm~~, which is 42.5 ppm higher than the WLG value for the same year.

Formatted: Font: Symbol

Formatted: Superscript

Formatted: Not Superscript/ Subscript

The ^{13}C/^{12}C ratio ~~^{13}C composition~~ of atmospheric CO_2 displayed a more clear~~larger~~ seasonal cycle than the mole fraction (Figure 2). The monthly mean value was (-9.07 ± 0.91)~~-9.07~~ ‰ and (-7.63 ± 0.97~~-7.63~~ ‰) for January and July, respectively, with a seasonal amplitude of 1.44 ‰. The mean value for the whole experimental period was -8.48 ‰, which is the same as the WLG value (-8.48 ‰). The summertime (June to ~~-~~August) δ^{13}C was 0.39 ‰ ~~more enriched~~ higher than the WLG background value.

The strongest di~~urnal~~el variation in the CO_2 mole fraction was observed in the autumn season (September to November) and the weakest in the winter season (December to February), with a di~~urna~~el amplitude of 27.9 µmol mol^{-1}~~ppm~~ and 13.4 µmol mol^{-1}~~ppm~~, respectively (Figure 3). In the summer season, the peak value was observed at 07:00 and the lowest value at 19:00. Contrary to the CO_2 mole fraction, δ^{13}C showed the lowest value in the early morning and the highest value in the afternoon in all the four seasons. The di~~urna~~el amplitude was 1.36 ‰ in the summer and 0.66 ‰ in the winter.

3.2 ^{13}C/^{12}C~~Isotop~~ ratio~~ic composition~~ of the surface sources (δ~~^{13}C~~s)

Figures 4 and 5 show an example of ~~Applying~~ the Miller-Tans approach applied to the month of January 2014. According to the slope parameter estimation, the ^{13}C/^{12}C ratio of the surface~~whole experimental period yielded an apparent~~ sources was~~signature of~~ (-25~~4~~.01~~75~~ ± 0.90~~26~~) ‰ (mean ± 95 % confidence limit~~bound~~) for ~~sources in~~ the YRD (Figure 4) and (-25.23~~4.24~~ ± 0.74~~21~~) ‰ for ~~sources in~~ Nanjing (Figure 5). ~~Strictly, this method is not accurate when applied over such an extensive period because the source signature varies seasonally, violating the condition of constant source signal under which the method can be used. So~~

Formatted: Superscript

Formatted: Superscript

Formatted: Superscript

Formatted: Superscript

Formatted: Superscript

Formatted: Superscript

~~these data plots are meant more to show the range of variations of the hourly observations than for determining the true annual mean source signatures.~~

Figure 6 shows the monthly isotopic ratio~~^{13}C signature~~ calculated with the Miller-Tans method for the ~~daytime and nighttime~~whole observation period. The reader is reminded here that the results obtained for the daytime and the nighttime period represent sources in the YRD and in Nanjing, respectively. During the two and a half years of observation, the monthly δ~~^{13}C~~$_S$ for the YRD was lower in the winter [(-24.37 ± 0.71) ‰] and higher in the summer [(-23.42 ± 1.79) ‰]. The seasonal difference for Nanjing was smaller than for the YRD [(-24.87 ± 0.51) ‰ in the winter (December to February) and -24.80 ± 1.79) ‰ in the summer months (June to August)]. ~~-~~The sources in the YRD had slightly higher δ_S ~~^{13}C compositions~~ than those in in Nanjing~~. The January mean value (mean of January 2014 and January 2015) was -24.13‰ and -24.78‰, and the mean value of the three August months was -20.67‰ and -22.76‰ for the YRD and Nanjing, respectively~~. The mean δ_S value of the whole observational period was (-24.37 ± 0.61)~~-23.26~~ ‰ and (-25.58 ± 0.44)~~-23.72~~ ‰ for the YRD and Nanjing, respectively. ~~These mean values based on the monthly analysis were 1.49‰ and 0.52‰ greater than the apparent source signatures derived from the application of the Miller-Tans method to the whole dataset (Figures 4 and 5).~~ The monthly δ~~^{13}C~~$_S$ for the YRD (Figure 6a) was highly correlated with the monthly atmospheric δ^{13}C [~~(~~Figure 2; δ_S = (2.29 ± 0.78) δ^{13}C + (-5.71±6.37), ~~-~~linear correlation coefficient = 0.47~~63~~, n = 30, p <0.0~~0~~1]~~)~~. The correlation between the monthly δ~~^{13}C~~$_S$ for Nanjing (Figure 6b) and the monthly atmospheric δ^{13}C was weak~~not as strong~~ [~~(~~δ_S = (2.39 ± 0.92) δ^{13}C + (-3.71 ± 8.07), linear correlation coefficient = 0.03~~26~~, n = 30, p = 0.87~~22~~]~~)~~. These correlation patterns suggest that

Formatted: Font: Symbol, Italic

Formatted: Subscript

atmospheric δ^{13}C was influenced more by surface sources at the regional scale than at the local (city) scale.

3.3 Inventory data for anthropogenic sources

The emission strength of anthropogenic sources and their ^{13}C/^{12}C~~isotopic~~ ratio~~signature~~ were calculated with the inventory method and the data found in the literature, as described in section 2.3. In the YRD, coal combustion was by far the largest source of anthropogenic CO_2, contributing 70 % of the overall “fossil-plus” emission (Table 2). Here the “fossil-plus” emission includes contributions from all forms of fossil fuel and from non-cement industrial processes. The second and third largest source were ammonia synthesis and pig iron, with fractional contributions of about 9 %. The “fossil-plus” source contribution to the total anthropogenic emission was 91 %, with the remaining 9 % contributed by cement production (Table 2).

In the Nanjing municipality, the fractional contribution of coal to the “fossil-plus” total was 52 %, lower than that for the YRD, and the other three major sources were ammonia synthesis (16 %), pig iron (13 %), and gasoline (11 %). The fractional contribution of fuel-plus sources to the total anthropogenic emission was 96.4 % and the fractional contribution of cement production was 3.6 % (Table 2). The isotopic ratio~~signature~~ of the “fossil-plus” sources was 0.35 ‰ lower for Nanjing than for the YRD.

The overall effective isotopic ratio~~signature~~ of the anthropogenic sources weighted by the source contributions was also lower for Nanjing than for the YRD (Table 3). The difference was 1.76 ‰ and was a result of lower fractional contributions in Nanjing of coal

Formatted: Superscript

Formatted: Superscript

combustion and cement production, which have relatively high ^{13}C contents, and a higher fractional contribution of natural gas, which is the fuel type with the lowest ^{13}C content.

3.4. CO_2 fluxes in YRD and Nanjing

Figure 7 shows the biological flux F_P and surface flux F_S calculated from the mass balance, and the cement flux F_C and "fossil-plus" F_F. The F_P flux obtained with the isotopic partitioning method for the YRD agreed with the seasonal phenology expected for plants in this region. It was near zero or slightly negative in the summer and generally positive in the winter, indicating uptake and release, respectively. The annual mean daytime biological flux was (-0.03 ±~~1~~ 0.64) mg m^{-2} s^{-1} in the YRD in the calendar year 2014. The net surface flux F_S was (0.17 ± 2.02) ~~0.16~~ mg m^{-2} s^{-1} in 2014. The standard deviations of these estimates are quite large. If the extreme standard deviations of F_p (5.16 mg m^{-2} s^{-1}) and F_S (22.00 mg m^{-2} s^{-1}) in March 2014 were excluded, the mean standard deviation of F_p would decrease to 0.23 mg m^{-2} s^{-1}for and that of F_S to 0.20 mg m^{-2} s^{-1}.

In Nanjing, the biological flux was positive throughout the year (Figure 8). This is because the partitioning was done for the night hours when the natural ecosystems were a source of CO_2 due to autotrophic and heterotrophic respiration. ~~The flux was greater in the summer than in the winter (Figure 8).~~ The annual mean nighttime biological flux for the calendar year 2014 was (0.06 ± 0.26) ~~0.03~~ mg m^{-2} s^{-1}. The nighttime surface flux was (0.18 ± 0.22) ~~0.16~~ mg m^{-2} s^{-1} in 2014.

4 Discussion

4.1 CO$_2$ mole fraction and δ^{13}C seasonality

The atmospheric CO$_2$ mole fraction observed in Nanjing showed very small seasonal variation (summer versus winter difference of 7.9 μmol mol^{-1} ~~ppm~~, July versus January difference of 15.6 μmol mol^{-1}~~ppm~~), in comparison with the data published for other cities. The CO$_2$ mole fraction difference between the cold and the warm season is about 66 μmol mol^{-1}~~ppm~~ in Phoenix, USA (Idso et al. 2002). In Salt Lake City, USA, the CO$_2$ mole fraction in the summer is about 31 μmol mol^{-1}~~ppm~~ lower than in the winter (Pataki et al., 2003). In Chicago, USA, the CO$_2$ mole fraction varied from 397 μmol mol^{-1}~~ppm~~ in August 2011 to 427 μmol mol^{-1}~~ppm~~ in January 2012, showing a seasonal amplitude of 30 μmol mol^{-1}~~ppm~~ (Moore and Jacobson 2015). In Beijing, China, the seasonal variation of atmospheric CO$_2$ mole fraction is about 64.5 μmol mol^{-1}~~ppm~~ (August versus January; Pang et al. 2016). However, a similar small seasonal amplitude of 5 μmol mol^{-1}~~ppm~~ CO$_2$ was observed in Pasadena, USA during 2006 to 2013, which was consistent with the seasonal variation of background and transport of emissions from fossil fuel combustion (Newman et al. 2016).~~which was consistence with the seasonal variation of background and emission from fossil fuel combustion (Miller et al. 2016).~~

Several factors contributed to the weak seasonality in Nanjing. The climate in the YRD is relatively mild. The governmental energy policy prohibits winter heating in public buildings. Most residential buildings also lack space heating in the winter. This is in contrast to energy use patterns in northern cities in China and elsewhere. In London, UK, natural gas usage in the winter heating season is 29 % greater than in the non-heating autumn season (Helfter et al. 2011). In Salt Lake City, USA, energy consumption in the winter was 41 %

Formatted: Font: Symbol

Formatted: Superscript

greater than in the summer (Bush et al, 2007). A similar seasonal trend of energy consumption has also been reported for Beijing (Pang et al, 2016). In Chicago, natural gas usage comprises ~~varied~~ 70 % to 80 % of total fossil fuel consumption in the winter and about 50 % in the summer (Moore and Jacobson 2015). The weak energy use seasonality in the YRD partially explains why the observed CO_2 mole fraction had a smaller seasonal amplitude (Figure 2) than reported for other northern cities.

The weak seasonality of the observed mole fraction was also related to the low vegetation cover in the YRD and in Nanjing. The forest cover ratio is about 35 % in Nanjing and in the YRD, and the overall vegetation cover (forest plus other vegetation types) ratio in the major cities in the YRD is lower than 45 % (CESY, 2013; CSY, 2013). For comparison, the vegetation cover ratio is 56 % in Salt Lake City (Pataki et al. 2009) and 44 % in Chicago (Rose et al. 2003). Dense vegetation is known to deplete atmospheric CO_2 in the summer season via photosynthetic uptake, amplifying the CO_2 seasonal amplitude.

Our $\delta^{13}C$ seasonal amplitude (January versus July difference 1.44 ‰) was 4 times the amplitude observed or estimated at WLG (Figure 2) but agreed with those reported by most urban studies. For comparison, the seasonal amplitude of $\delta^{13}C_a$ in Bangalore, India, was 0.89 to 1.32 ‰ (Guha and Ghosh 2015). Similar amplitudes have also been reported for Chicago (January versus August difference 1.25 ‰; Moore and Jacobson, 2015) and Beijing (2.13 ‰; Pang et al. 2016). In Salt Lake City, the seasonal amplitude of $\delta^{13}C$ was approximately 1.6 ‰ because of much more natural gas consumption for heating in the winter than in the summer (Pataki et al. 2006).

4.2 Influences of cement production on atmospheric δ^{13}C

The high summer δ^{13}C was one of the most unique characteristics at our site. The daytime δ^{13}C reached -6.90 ‰ in July 2013 and -7.21 ‰ in August 2014, which were 1.28 ‰ and 0.95 ‰ higher than the WLG values. The highest monthly mean δ^{13}C occurred in July: -7.44 ‰ in July 2013, -7.99 ‰ in July 2014 and -7.46 ‰ in July 2015. These values were 0.74 ‰, 0.16 ‰ and 0.77 ‰ higher than the WLG value reported for the same months.

The high July values observed at our site cannot be fully explained by CO_2 removal by plant photosynthesis. Photosynthesis and respiration are the two processes that dominate the ^{13}C/^{12}C seasonality in plant-dominated landscapes, leading to higher δ^{13}C values in the summer and lower values in the winter. For example, in Park Falls, Wisconsin, USA, a site in a heavily-forested landscape, δ^{13}C was -7.75 ‰ in August 2011 and -8.77 ‰ in February 2012 (Moore and Jacobson, 2015). For comparison, δ^{13}C was -8.24‰ and -8.38 ‰ at the Mauna Loa Observatory and -8.02 ‰ and -8.66 ‰ at WLG in these two months, respectively. In other words, the photosynthetic effect raised the August δ^{13}C by 0.5 ‰ above the background value, a smaller enrichment than observed at our site. Because of the low vegetation fraction, the summer photosynthetic CO_2 uptake in the YRD and in Nanjing should be lower than at Park Falls. According to the Carbon~~-~~Tracker inversion analysis (Peters et al. 2007), the net ecosystem production at the grid point where Parks Fall is located is -0.201 mg m^{-2} s^{-1} in July, 2014 but is only -0.059 mg m^{-2} s^{-1} at the grid point corresponding to the YRD region. We would expect from the photosynthetic effect alone that the summertime ^{13}C enrichment at our site to be smaller, not greater than that observed at Park~~s~~ Falls.

Formatted: Superscript

Furthermore, in a human-dominated landscape, the plant photosynthetic enhancement of ^{13}C is offset by the CO_2 from fossil fuel combustion which has lower ^{13}C/^{12}C ratios than the atmosphere~~contents~~. In Chicago, the monthly mean δ^{13}C peaked in August at -8.29 ‰ during the calendar year 2011, which is 0.05 ‰ lower than the WLG value for the same month. Similarly, in Beijing, the monthly mean δ^{13}C peaked at -9.49 ‰ in August 2014, which is 1.23 ‰ lower than the WLG value for the same month.

We suggest that cement production was the contributing factor responsible for the high δ^{13}C values in the summer. The evidence supporting this interpretation is provided by data in Table 3 and Figure 7. The ~~δ^{13}C signal~~delta value of anthropogenic CO_2 in the YRD would be (-26.36 ± 0.42)~~-26.42~~ ‰ without cement production and increased to (-23.95 ± 0.41)~~-23.71~~ ‰ after inclusion of the cement source (Table 3). This delta ~~δ^{13}~~C value is much higher than those reported for other urban lands, such as -30.7 ‰ for Los Angeles, USA (Newman et al. 2008) and about -31 ‰ for Salt Lake City, USA (Bush et al. 2007). The overall surface source ^{13}C/^{12}C~~–~~ ratio~~signal~~ derived from atmospheric measurements (Figure 6;~~,~~ -24.37 ‰ and -24.58 ‰~~-23.26‰ and -23.72‰~~ for the YRD and Nanjing, respectively) was also more enriched than those obtained from atmospheric measurements in other cities, such as (-28.1 ± 0.8) ‰ for Chicago in August and September (Moore and Jacobson, 2015), -32.4 ‰ to -27.4 ‰ for Salt Lake City in the growing season (Pataki et al. 2003), -27.0~~0~~ ‰ for Beijing in the winter heating season (Pang et al. 2016), and -29.3 ‰ for Los Angeles, USA (Newman et al. 2008).

The influence of cement production on atmospheric δ^{13}C has also been suggested for at least two other urban sites. In Bangalore, India, δ^{13}C is 0.05 ‰ higher than that observed at

Formatted: Superscript

Formatted: Font: 12 pt

Formatted: Font: 12 pt

Formatted: Superscript

Formatted: Superscript

an island station in the Indian Ocean, and cement production in southern India is offered as a reason to explain the enrichment of urban δ^{13}C (Guha and Ghosh 2015). The other urban site is Beijing, China, where the δ^{13}C measurement may have been influenced by cement factories outside the city (Ren et al. 2015, Pang et al. 2016).

4.3 Net surface and biological fluxes in the YRD

As a human-dominated landscape, the YRD was a net source of CO_2 on the monthly scale even in the growing season (F_S, Figure 7). The seasonal trends of the net surface flux F_S and the biological flux F_P were highly correlated with each other because the anthropogenic source strengths were almost constant. The mean F_S between March 2013 and February 2015 was (0.19 ± 1.16) ~~0.17~~ mg $m^{-2} s^{-1}$, which consisted of (0.15~~6~~ ± 0.02) mg $m^{-2} s^{-1}$ from fossil combustion and industrial processes, (0.02 ± 0.002) mg $m^{-2} s^{-1}$ from cement production and (0.05 ± 1.31) ~~0.01~~ mg $m^{-2} s^{-1}$ from biological activities. The total anthropogenic CO_2 flux was (0.17± 0.02) ~~8~~ mg $m^{-2} s^{-1}$ in the YRD, a 70~~67~~ % increase from the value of 0.10 mg $m^{-2} s^{-1}$ reported for 2009 (Shen et al. 2014). From 2009 to 2012, the GDP increased by 56 % according to the National Statistic Yearbook.

For comparison, we extracted the flux data from the Carbon-Tracker database for the 6 by 6 pixels that cover the YRD region. The results show that the mean daytime (11:00 to 17:00 local time) biological flux is slightly negative at -0.014 mg $m^{-2} s^{-1}$ for 2014 (Peter et al. 2007). Our estimate of F_P for 2014 was (0.03 ± 0.64) mg $m^{-2} s^{-1}$. As pointed out earlier, the F_P value for March 2014 was highly uncertain [(0.21± 5.16) mg $m^{-2} s^{-1}$]; If we replace this value by the mean value of February and April 2014, the 2014 mean F_P ~~also indicates that the~~

Formatted: Subscript

Formatted: Subscript

~~region was a negligibly small biological sink of CO$_2$~~would be reduced to ~~(~~(0.02 ± 0.22) ~~-0.009~~ mg m^{-2} s^{-1}~~)~~.

~~We conducted Monte Carlo simulations to assess the sensitivity of the partitioned fluxes to uncertainties in $\delta^{13}C_P$ and $\delta^{13}C_F$. Errors in these parameters were assumed to follow a uniform distribution and varied in the range of ±1‰. The mean and standard deviation of F_S were 0.167 and 0.003 mg m^{-2}s^{-1}, and those of F_P were -0.005 and 0.003 mg m^{-2}s^{-1}, respectively for the YRD, based on an ensemble of 10,000 simulations. For Nanjing, the mean ± standard deviation of F_S and F_P was 0.209 ± 0.024 and 0.086 ± 0.022 mg m^{-2}s, respectively. These mean flux values are essentially the same as those obtained with the default $\delta^{13}C_P$ and $\delta^{13}C_F$ values giving in Table 3 and the standard deviations represent uncertainties of the partitioned fluxes.~~

A~~nother~~ source of uncertainty in our flux partitioning analysis is related to human breath (Affek and Eiler 2006). Using the method of Prairie and Duarte (2007), we estimated that human respiration flux was 0.006 and 0.013 mg m^{-2} s^{-1}, or 3.7 % and 11.65 % of anthropogenic emission in the YRD and in Nanjing, respectively. The food diet in the region is predominantly C3 grains. By including this additional source in Equations 3 and 4 and by assuming that the isotopic ratio~~signature~~ of human respiration is the same as δ~~^{13}C~~$_P$ shown in Table 3, F_S and F_P would increase by 0.008 and 0.001 mg m^{-2} s^{-1} in the YRD and by 0.018 mg m^{-2} s^{-1} and 0.005 mg m^{-2} s^{-1} in Nanjing, respectively.

4.4 Comparison of the Miller-Tans and the Keeling method

By applying the Miller-Tans method to daytime and nighttime observations separately, we obtained the effective source ratio~~signature~~s that are consistent with the inventory analysis for the YRD and for the Nanjing Municipality. The daytime measurement revealed that the $^{13}C/^{12}C$ ratio of the sources were on average 0.241~~6~~ ‰ higher than ~~more enriched~~that~~ in ^{13}C than the signature $\delta^{13}C_S$~~ obtained with the nighttime measurement. For comparison, the overall $\delta^{13}C_S$ of the anthropogenic sources in the YRD was also higher than that in Nanjing, the difference being 2~~1~~.01~~76~~ ‰ (Table 2). The interpretation that the daytime observations capture the influence of surface sources in the YRD region is supported by a trajectory analysis and by an analysis of the atmospheric methane to CO_2 emissions ratio observed at the same site (Shen et al. 2014). We note that the atmospheric measurements gave a smaller difference between the YRD and Nanjing than that obtained by the inventory data, likely because of different biological contributions between the two spatial scales.

Formatted: Superscript

Formatted: Superscript

We also calculated the $^{13}C/^{12}C$ ratio of the surface sources with the~~We argue that~~ Keeling plot method. Using the daytime data, the Keeling result was lower and more variable than that inferred from the Miller-Tans method using the daytime data (Figure 6a). ~~is not appropriate for daytime periods because the surface air is influenced by both the surface sources and by entrainment of the background air from above the boundary layer. If we applied the Keeling method to the daytime observations, the linear correlation coefficient was on average -0.898 which is weaker than the correlation coefficient obtained with the Miller-Tans method (-0.956).~~ The~~ resulting mean $\delta^{13}C_S$ –~~ two methods differed by an average of~~would be~~ -1.51~~0.61~~ ‰ (Supplementary Table S2)~~ lower than the mean value shown in~~

Formatted: Superscript

Formatted: Superscript

~~Figure 6~~. ~~The difference in $\delta^{13}C_S$ between the YRD (daytime observations, Keeling method) and Nanjing (nighttime observations, Miller-Tans method) would become too small (0.15‰).~~

In comparison, the Keeling plot method showed reasonably good performance when applied to the nighttime observations. This is because surface inversion conditions effectively prevented mixing of the free atmospheric air with the surface air, so that the single-source assumption implicit in the Keeling plot method could be~~was~~ satisfied. If we applied Keeling plot method at monthly intervals to the nighttime data, the resulting δ~~^{13}C~~$_S$ showed very similar month-to-month variations with ~~would decrease to -24.24‰ for Nanjing from -23.72‰,~~ the value obtained with application of the Miller-Tans method to the nighttime observations (Figure 6b). The two method differed by an average of 0.21 ‰ (Supplementary Table S2).

5. Conclusion

We showed that the temporal changes of $\delta^{13}C$ followed the seasonal patterns of anthropogenic and biologic CO_2 emissions, with lower values in the winter than in the summer. An unusual feature that has not been seen in other urban environments is that the $\delta^{13}C$ exceeded that of the background atmosphere in some of the summer months. The highest monthly $\delta^{13}C$ was -7.44 ‰ observed in July 2013, which was 0.74 ‰ greater than the WLG value for the same month. Evidence points to cement production as the key reason for why the atmospheric $\delta^{13}C$ was higher than at the background site. In contrast to the isotope ratio~~^{13}C signal~~, the CO_2 mole fraction displayed very weak seasonality (July to January difference 15.6 μmol mol^{-1}~~ppm~~).

Formatted: Font: Symbol

Formatted: Superscript

We hypothesized that the Miller-Tans method applied to the daytime and nighttime observations should yield the effective $^{13}C/^{12}C$ ~~isotopic~~ ratio~~signature~~ of surface sources at the regional (YRD) and the local (Nanjing) scale, respectively. According to the results of the Miller-Tans method, the effective source $^{13}C/^{12}C$ ratio~~signal~~ in the YRD was -24.37 ‰~~-23.25‰~~, which was 0.21~~46~~ ‰ higher than that in the Nanjing Municipality. These results were consistent with inventory estimates of anthropogenic source ratio~~signature~~s at these two spatial scales.

Formatted: Superscript

Formatted: Superscript

By combining inventory data on anthropogenic carbon~~C~~ sources and the atmospheric measurement of CO_2 mole fraction and ~~its~~ $^{13}C/^{12}C$ ratio ~~^{13}C composition~~ in an isotopic partitioning framework, we inferred that natural ecosystems in the YRD were a negligibly small source ~~sink~~ of atmospheric CO_2, with an average flux of (0.02 ± 0.22) mg m^{-2} s^{-1} ~~0.009 mg $m^{-2}s^{-1}$~~ for 2014.~~.~~ For comparison, t~~T~~he Carbon-Tracker inverse analysis ~~also~~ reveals a small annual mean daytime biological flux (-0.014 mg m^{-2} s^{-1}) for this region for 2014.

Formatted: Superscript

Formatted: Superscript

Data availability:

The atmospheric data are available upon request and from the Yale-NUIST Center website http://yncenter.sites.yale.edu/publications.

Acknowledgments:

This research was supported by the National Natural Science Foundation of China (Grant 41475141, 41505005), the U. S. National Science Foundation (Grant 1520684), the Ministry of Education of China (Grant PCSIRT), and the Priority Academic Program Development of

Jiangsu Higher Education Institutions (Grant PAPD). The first author also acknowledged a visiting scholarship from China Scholarship Council and a Graduate Student Innovation Grant from Jiangsu Provincial Government (Grant KYLX_0848). We thank the handling editor Dr. Jan Kaiser and three anonymous reviewers whose constructive comments have greatly improved this paper.

References

Affek, H. P., Eiler, J. M. (2006). Abundance of mass 47-~~-~~CO_2 in urban air, car exhaust, and human breath. Geochimica et Cosmochimica Acta **70**(1): 1-12.

Formatted: Subscript

Akbari H, Menon S, Rosenfeld A. Global cooling: increasing world-wide urban albedos to offset CO_2. Climatic Change, 2009, **94**(3-4): 275-286.

Formatted: Subscript

An, H (2012) Ammonia synthesis: current status and future outlook (in Chinese), Coal Chemsitry of Western China, **2**: 4-13.

Formatted: Font: Bold

Andres, R. J., Marland, G., Boden, T., Bischof, S. (1994). Carbon dioxide emissions from fossil fuel consumption and cement manufacture, 1751-1991; and an estimate of their isotopic composition and latitudinal distribution, Oak Ridge National Lab., TN (United States);

Bai, Y., (2011) A C~~c~~omparative S~~s~~tudy on T~~t~~urbulent F~~f~~luxes E~~e~~xchange over Nanjing U~~u~~rban and S~~s~~uburban in S~~s~~ummer~~.~~ (i~~i~~n Chinese)~~ Nanjing~~, Master’s Thesis, Nanjing University of Information Science & Technology.

Ballantyne, A. P., Miller, J. B., Baker, I. T., Tans, P. P., White, J. W. C. (2011). Novel applications of carbon isotopes in atmospheric CO_2: what can atmospheric measurements teach us about processes in the biosphere?~~.~~ Biogeosciences, 8(10), 3093-3106.

Formatted: Subscript

Ballantyne, A. P., Miller, J. B., Tans, P. P. (2010). Apparent seasonal cycle in isotopic discrimination of carbon in the atmosphere and biosphere due to vapor pressure deficit. Global Biogeochemical Cycles, 24(3), 1-16.

Bowling, D. R., S P Burns, T. J. Conway, R. K. Monson, and J. W. C. White (2005) Extensive observations of CO_2 carbon isotope content in and above a high-elevation subalpine forest, Global Biogeochemical Cycles, **19**: GB3023.

Formatted: Subscript

Formatted: Font: Bold

Bi, J., Zhang, R., Wang, H., Liu, M.,Wu, Y. (2011). The benchmarks of carbon emissions and policy implications for China's cities: Case of Nanjing. Energy Policy **39**(9): 4785-4794.

Bowling, D. R., Sargent, S. D., Tanner, B. D., and Ehleringer, J. R. (2003). Tunable diode laser absorption spectroscopy for stable isotope studies of ecosystem–atmosphere CO_2 exchange, Agric. Forest Meteorol., **118:** 1–19.

Formatted: Subscript

Bush, S. E., Pataki, D.E., Ehleringer, J.R. (2007). Sources of variation in $\delta^{13}C$ of fossil fuel emissions in Salt Lake City, USA. Applied Geochemistry **22**(4): 715-723.

Formatted: Superscript

CESY (2013). China Energy Statistical Yearbook 2013: China Statistical Publishing House, Beijing. (in Chinese) Also available at: <http://www.stats.gov.cn/tjsj/ndsj/2013/indexch.htm>.

Clark-Thorne, S. T., C. J. Yapp (2003). Stable carbon isotope constraints on mixing and mass balance of CO2 in an urban atmosphere: Dallas metropolitan area, Texas, USA. Applied Geochemistry **18**(1): 75-95.

Coutts, A. M., Beringer, J., Tapper, N.J. (2007). Characteristics influencing the variability of urban CO_2 fluxes in Melbourne, Australia. Atmospheric Environment **41**(1): 51-62.

Formatted: Subscript

China Cement: http://hy.ccement.com/map/, last access: 6 July 2016 (in Chinese).

CSY (2013). China Statistical Yearbook. National Bureau of Statistics of China. (in Chinese) Also available at: <http://www.stats.gov.cn/tjsj/ndsj/2013/indexch.htm>

Duan Y. (1995) Study of characteristics of coal isotope conposition in China. Coal Geology & Exploration **23**(1) 29-33.

Ehleringer, J.R., Bowling, D.R., Flanagan, L.B., Fessenden, J.,Helliker, B., Martinelli, L.A., Ometto, J.P. (2002). Stable isotopes and carbon cycle processes in forests and grasslands. Plant biology **4**(2): 181-189.

Farquhar, G., J. Lloyd (1993). Carbon and oxygen isotope effects in the exchange of carbon dioxide between terrestrial plants and the atmosphere. Stable isotopes and plant carbon-water relations **40**: 47-70.

Fessenden, J. E., J. R. Ehleringer (2002). Age-related variations in $\delta^{13}C$ of ecosystem respiration across a coniferous forest chronosequence in the Pacific Northwest. Tree Physiology **22**(2-3): 159-167.

Formatted: Superscript

Friedman, L., A. P. Irsa (1967). Variations in isotopic composition of carbon in urban atmospheric carbon dioxide. Science **158**(3798): 263-264.

Gorski G, Strong C, Good S P, Bares, R., Ehleringer, J. R., Bowen, G. J. (2015). Vapor hydrogen and oxygen isotopes reflect water of combustion in the urban atmosphere. Proceedings of the National Academy of Sciences, ~~2015,~~ **112**(11): 3247-3252.

Griffis, T. J., Lee, X., Baker, J.M., Sargent, S.D., King, J.Y. (2005). Feasibility of quantifying ecosystem–atmosphere $C^{18}O^{16}O$ exchange using laser spectroscopy and the flux-gradient method. Agricultural and Forest Meteorology, **135**(1-4): 44-60.

Formatted: Superscript

Formatted: Superscript

Griffis, T J. (2013). Tracing the flow of carbon dioxide and water vapor between the biosphere and atmosphere: A review of optical isotope techniques and their application. Agricultural and Forest Meteorology, **174**:85-109.

Guha, T., P. Ghosh (2010). Diurnal variation of atmospheric CO$_2$ concentration and delta C-13 in an urban atmosphere during winter-role of the n~~N~~octurnal b~~B~~oundary l~~L~~ayer. Journal of Atmospheric Chemistry, **65**(1): 1-12.

Formatted: Subscript

Guha, T. and P. Ghosh (2015). Diurnal and seasonal variation of mixing ratio and delta C-13 of air CO$_2$ observed at an urban station Bangalore, India. Environmental Science and Pollution Research, **22**(3): 1877-1890.

Formatted: Subscript

Helfter, C., Famulari, D., Phillips, G.J., Barlow, J.F., Wood, C.R.,Grimmond, C.S.B., Nemitz, E. (2011). Controls of carbon dioxide concentrations and fluxes above central London. Atmospheric Chemistry and Physics **11**(5): 1913-1928.

ICLEI (International Council for Local Environmental Initiatives). (2008). Local government operations protocol for the quantification and reporting of greenhouse gas emissions inventories. [Available online at http://www.arb.ca.gov/cc/protocols/localgov/archive/final lgo protocol 2008–09–25.pdf.]

Idso, S. B., Idso, C.D., Balling, R.C. (2002). Seasonal and diurnal variations of near-surface atmospheric CO$_2$ concentration within a residential sector of the urban CO$_2$ dome of Phoenix, AZ, USA. Atmospheric Environment, **36**(10): 1655-1660.

Formatted: Subscript

Formatted: Subscript

Jasek, A., Zimnoch, M., Gorczyca, Z., Smula, E., Rozanski, K. (2014). Seasonal variability of soil CO2 flux and its carbon isotope composition in Krakow urban area, Southern Poland. Isotopes in Environmental and Health Studies, **50**(2): 143-155.

Keeling, C. D. (1958). The concentration and isotopic abundances of atmospheric carbon dioxide in rural areas. Geochimica et Cosmochimica Acta, **13**(4): 322-334.

Keeling, C. D. (1961). The concentration and isotopic abundances of carbon dioxide in rural and marine air. Geochimica et Cosmochimica Acta, **24**(3): 277-298.

Koerner, B., J. Klopatek (2002). Anthropogenic and natural CO$_2$ emission sources in an arid urban environment. Environmental Pollution, **116**: S45-S51.

Formatted: Subscript

Leavitt, S. W., Paul, E.A., Galadima, A., Nakayama, F.S., Danzer, S.R., Johnson, H., Kimball, B.A. (1995). Carbon isotopes and carbon turnover in cotton and wheat FACE experiments. Plant and Soil **187**(2): 147-155.

Lichtfouse, E., Lichtfouse, M., Jaffrezic, A. (2003). delta C-13 values of grasses as a novel indicator of pollution by fossil-fuel-derived greenhouse gas CO_2 in urban areas. Environmental Science & Technology, **37**(1): 87-89.

Formatted: Subscript

Liu, H., Feng, J., Järvi, L., Vesala, T. (2012). Four-year (2006–2009) eddy covariance measurements of CO_2 flux over an urban area in Beijing. Atmospheric Chemistry and Physics, **12**(17): 7881-7892.

Formatted: Subscript

Lloyd, J., Kruijt, B., Hollinger, D.Y., Grace, J., Francey, R.J., Wong, S., Kelliher, F.M., Miranda, A.C., Farquhar, G.D., Gash, J.H.C. (1996). Vegetation effects on the isotopic composition of atmospheric CO_2 at local and regional scales: theoretical aspects and a comparison between rain forest in Amazonia and a boreal forest in Siberia. Functional Plant Biology, **23**(3): 371-399.

Formatted: Subscript

Lloyd, J., Francey, R.J., Mollicone, D., Raupach, M.R, Sogachev, A., Arneth, A., Byers, J.N., Kelliher, F.M., Rebmann, C., Valentini, R. (2001). Vertical profiles, boundary layer budgets, and regional flux estimates for CO_2 and its ^{13}C/^{12}C ratio and for water vapor above a forest/bog mosaic in central Siberia. Global Biogeochemical Cycles, **15**(2): 267-284.

Formatted: Subscript

Formatted: Superscript

Formatted: Superscript

McDonald, B.C., McBride, Z. C., Martin, E. W., Harley, R. A. (2014). High-resolution mapping of motor vehicle carbon dioxide emissions. Journal of Geophysical Research: Atmospheres,~~ 2014,~~ **119**(9): 5283-5298.

McManus, J. B., Zahniser, M.S., Nelson, D.D., Williams, L.R., Kolb, C.E. (2002). Infrared laser spectrometer with balanced absorption for measurement of isotopic ratios of carbon gases. Spectrochimica Acta Part A: Molecular and Biomolecular Spectroscopy, **58**(11): 2465-2479.

Miller, J. B., P. P. Tans (2003). Calculating isotopic fractionation from atmospheric measurements at various scales,~~.~~ Tellus B, **55**(2): 207-214.

Miller, J.B., Tans, P.P., White, J.W.C., Conway, T.J., Vaughn, B.W. (2003). The atmospheric signal of terrestrial carbon isotopic discrimination and its implication for partitioning carbon fluxes,~~.~~ Tellus B, **55**(2): 197-206.

Newman, S., Xu, X., Gurney, K.R., Hsu, Y.K., Li, K.F., Jiang, X., Keeling, R., Feng, S., O'Keefe, D., Patarasuk, R. and Wong, K.W. (2016). Toward consistency between trends in bottom-up CO_2 emissions and top-down atmospheric measurements in the Los Angeles megacity. Atmospheric Chemistry and Physics, **16**(6):3843-3863.

Formatted: Subscript

Formatted: Font: Bold

Moore J., Jacobson A.D. (2015). Seasonally varying contributions to urban CO_2 in the Chicago, Illinois, USA region: Insights from a high-resolution CO_2 concentration and d^{13}C record. Elementa: Science of the Anthropocene, **3**:~~,~~ 000052.

Formatted: Subscript

Formatted: Subscript

Formatted: Superscript

Mu, H., Li, H., Zhang, M., Li, M. (2013). Analysis of China's carbon dioxide flow for 2008. Energy Policy **54**: 320-326.

Newman, S., Xu, X., Affek, H.P., Stolper, E., Epstein, S. (2008). Changes in mixing ratio and isotopic composition of CO2in urban air from the Los Angeles basin, California, between 1972 and 2003,~~.~~ Journal of Geophysical Research, **113**(D23)~~.~~: 1-15.

NSY (2013). Nanjing Statistical Yearbook. Nanjing Municipal Bureau Statistics. (in Chinese) Also available at: < http://www.njtj.gov.cn/2004/2013/renmin/index.htm>

Ometto, J. P., Flanagan, L.B., Martinelli, L.A., Moreira, M.Z., Higuchi, N., Ehleringer, J.R. (2002). Carbon isotope discrimination in forest and pasture ecosystems of the Amazon Basin, Brazil,~~.~~ Global Biogeochemical Cycles, **16**(4):1-10.

Ometto, J.P., Ehleringer, J.R., Domingues, T.F., Berry, J.A., Ishida, F.Y., Mazzi, E., Higuchi, N., Flanagan, L.B., Nardoto, G.B., Martinelli, L.A. (2006). The stable carbon and nitrogen isotopic composition of vegetation in tropical forests of the Amazon Basin, Brazil,~~.~~ Biogeochemistry, **79**(1-2): 251-274.

Pan, J. (2007) Theoretical and Process Studies of the Abatement of Fuel Gas Emissions during Iron Ore Sintering (in Chinese), PhD Dissertation, Southcentral Univeristy of China.

Pang, J., Wen, X., Sun, X. (2016). Mixing ratio and carbon isotopic composition investigation of atmospheric CO_2 in Beijing, China. Sci Total Environ, **539**: 322-330.

Formatted: Subscript

Pataki, D. E. (2005). Can carbon dioxide be used as a tracer of urban atmospheric transport? Journal of Geophysical Research **110**(D15102)~~.~~: 1-8.

Pataki, D. E., Bowling, D.R., Ehleringer, J.R. (2003). Seasonal cycle of carbon dioxide and its isotopic composition in an urban atmosphere: Anthropogenic and biogenic effects. Journal of Geophysical Research-Atmospheres, **108**(D23)~~.~~: 1-8.

Pataki, D. E., Bowling, D.R., Ehleringer, J.R., Zobitz, J.M. (2006). High resolution atmospheric monitoring of urban carbon dioxide sources. Geophysical Research Letters, **33**(3)~~.~~: ~~:~~1-5.

Pataki, D. E., Ehleringer, J.R., Flanagan, L.B., Yakir, D., Bowling, D.R., Still, C.J., Buchmann, N., Kaplan, J.O., Berry, J.A. (2003). The application and interpretation of Keeling plots in terrestrial carbon cycle research. Global Biogeochemical Cycles, **17**(1): 1-14

Pataki, D. E., Lai, C., Keeling, C.D., Ehleringer, J.R. (2007). Insights from stable isotopes on the role of terrestrial ecosystems in the global carbon cycle. Terrestrial Ecosystems in a Changing World, Springer:~~:~~ 37-44.

Pataki,D.E., Emmi,P.C., Forster,C.B., Mills,J.I., Pardyjak,E.R., Peterson,T.R., Thompson,J.D., Dudley-Murphy,E., An integrated approach to improving fossil fuel emissions scenarios with urban ecosystem studies. Ecological Complexity, 2009, **6**(1): 1-14.

Pataki, D. E., Xu, T., Luo, Y.Q., Ehleringer, J.R. (2007). Inferring biogenic and anthropogenic carbon dioxide sources across an urban to rural gradient. Oecologia **152**(2): 307-322.

Peters,W., Jacobson, A.R., Sweeney, C., Andrews, A.E., Conway, T.J., Masarie, ~~,~~K., Miller, J.B., Bruhwiler, L.M., Petron, G., Hirsch, A.I., Worthy, D.E., van der Werf, G.R., Randerson, J.T., Wennberg, P.O., Krol, M.C., Tans, P.P. (2007)~~,~~ An atmospheric perspective on North American carbon dioxide exchange: CarbonTracker, ~~.~~Proceedings of the National Academy of Sciences, ~~2007,~~ **104**(48): 18925-18930.

Prairie, Yves T., ~~and Carlos M.~~ Duarte, ~~.~~C. M. (2007). ~~–~~Direct and indirect metabolic CO_2 release by humanity. ~~-~~ Biogeosciences, **4**(2): 215-217.

Rella, C. (2011). Accurate stable carbon isotope ratio measurements with rapidly varying carbon dioxide concentrations using the Picarro $\delta^{13}C$ G2101-i gas analyzer, Picarro White Paper. Picarro Inc.

Ren, L., Wang, W., Wang, J., Liu, R. (2015). Analysis of energy consumption and carbon emission during the urbanization of Shandong Province, China. Journal of Cleaner Production, **103**: 534-541.

Formatted: Font color: Text 1

Formatted: Font color: Text 1

Formatted: Font color: Text 1

Formatted: Font color: Text 1

Formatted: Font color: Text 1

Formatted: Font color: Text 1

Formatted: Font: Bold, Font color: Text 1

Formatted: Font color: Text 1

Formatted: Superscript

Röckmann1 T, S Eyer, C. van der Veen1, ME Popa, B Tuzson, G Monteil1, S Houweling, Eliza Harris, D Brunner, H Fischer, G Zazzeri, D Lowry, EG Nisbet, WA Brand, JM Necki, L Emmenegger, and J Mohn (2016). In situ observations of the isotopic composition of methane at the Cabauw tall tower site. Atmos. Chem. Phys., **16**: 10469–10487.

Formatted: Font: Bold

Rose L S, Akbari H, Taha H. Characterizing the fabric of the urban environment: a case study of Greater Houston, Texas. Lawrence Berkeley National Laboratory, 2003.

Satterthwaite D. Cities' contribution to global warming: notes on the allocation of greenhouse gas emissions. Environment and Urbanization, 2008, **20**(2): 539–549.

Shen, S., Yang, D., Xiao, W., Liu, S., Lee, X. (2014). Constraining anthropogenic CH_4 emissions in Nanjing and the Yangtze River Delta, China, using atmospheric CO_2 and CH_4 mixing ratios, ~~-~~ Advances in Atmospheric Sciences, **31**(6): 1343-1352.

Formatted: Subscript

Formatted: Subscript

Formatted: Subscript

Song, T., Wang Y. (2012). Carbon dioxide fluxes from an urban area in Beijing. Atmospheric Research, **106**: 139-149.

Sun, B., Dilcher, D.L., Beerling, D.J., Zhang, C., Yan, D., Kowalski, E. (2003). Variation in Ginkgo biloba L. leaf characters across a climatic gradient in China. Proceedings of the National Academy of Sciences, **100**(12): 7141-7146.

Takahashi, H. A., Konohira, E., Hiyama, T., Minami, M., Nakamura, T., Yoshida, N. (2002). Diurnal variation of CO_2 concentration, Delta C-14 and delta C-13 in an urban forest: estimate of the anthropogenic and biogenic CO_2 contributions,~~-~~ Tellus B, **54**(2): 97-109.

Tans, P. (1981). $^{13}C/^{12}C$ of industrial CO~~0~~^{2}. In SCOPE 16: Carbon Qcle Modelling (B.Bolin, ed.), John Wiley and Sons, Chichester, England, 127-129.

Thoning, K. W., Tans, P.P., Komhyr, W.D. (1989). Atmospheric carbon dioxide at Mauna Loa Observatory: 2. Analysis of the NOAA GMCC data, 1974–1985. Journal of Geophysical Research~~: Atmospheres, (1984–2012)~~ **94**(D6): 8549-8565.

Turnbull, J. C., Sweeney, C., Karion, A., Newberger, T., Lehman, S. J., Tans, P.P., Davis, K.J., Lauvaux, T., Miles, N.L., Richardson, S.J., Cambaliza. (2015). Toward quantification and source sector identification of fossil fuel CO_2 emissions from an urban area: Results from the INFLUX experiment. Journal of Geophysical Research~~: Atmospheres~~, 120(1):~~,~~ 292-312.

Sanam Noreen Vardag, S. N., S. Hammer, I. Levin (2016) Evaluation of 4 years of continuous $^{13}C(CO_2)$ data using a moving Keeling plot method, Biogeosciences, Biogeosciences, **13**: 4237–4251.

Wada, R., Nakayama, T., Matsumi, Y., Hiyama, T., Inoue, G., Shibata, T. (2011). Observation of carbon and oxygen isotopic compositions of CO_2 at an urban site in Nagoya using Mid-IR laser absorption spectroscopy. Atmospheric Environment, **45**(5): 1168-1174.

Wang, D. (2013) Method and Empirical Research of Urban Greenhouse Gas Measurement (in Chinese), Master's Thesis, Tianjin University.

Wang, W. , D. E. Pataki (2012). Drivers of spatial variability in urban plant and soil isotopic composition in the Los Angeles basin. Plant and Soil, **350**(1-2): 323-338.

Wen, X. F., Meng, Y., Zhang, X., Sun, X., Lee, X. (2013). Evaluating calibration strategies for isotope ratio infrared spectroscopy for atmospheric $^{13}CO_2/^{12}CO_2$ measurement. Atmospheric Measurement Techniques,~~ Discussions~~ **6**(1): 795-823.

Wehr, R., and S. R. Saleska (2017) The long-solved problem of the best-fit straight line: application to isotopic mixing lines, Biogeosciences, **14**: 17-29.

Widory, D. (2006). Combustibles, fuels and their combustion products: A view through carbon isotopes. Combustion Theory and Modelling, **10**(5): 831-841.

Formatted: Subscript

Formatted: Subscript

Formatted: Superscript

Formatted: Superscript

Formatted: Superscript

Formatted: Subscript

Formatted: Superscript

Formatted: Subscript

Formatted: Font: Bold

Formatted: Subscript

Formatted: Font: Bold

Widory, D., M. Javoy (2003). The carbon isotope composition of atmospheric CO_2 in Paris. Earth and Planetary Science Letters, **215**(1-2): 289-298.

Yakir, D., L. da SL Sternberg (2000). The use of stable isotopes to study ecosystem gas exchange. Oecologia, **123**(3): 297-311.

Yang, H.M., Wang, H.Z. , Wu, Y.B. (2011). Observation and characteristics analysis of traffic flow in Nanjing. (in Chinese), Environmental Science and Technology, **24**(2): 98-101.

Zimnoch, M., Florkowski, T., Necki, J., Neubert, R. (2004). Diurnal variability of delta C-13 and delta O-18 of atmospheric CO_2 in the urban atmosphere of Krakow, Poland,~~.~~ Isotopes in Environmental and Health Studies, **40**(2): 129-143.

Zobitz, J. M., Burns, S.P., Reichstein, M., Bowling, D.R. (2008). Partitioning net ecosystem carbon exchange and the carbon isotopic disequilibrium in a subalpine forest. Global Change Biology, **14**(8): 1785-1800.

Zondervan, A., H. A. Meijer (1996). Isotopic characterisation of CO_2 sources during regional pollution events using isotopic and radiocarbon analysis. Tellus B, **48**(4): 601-612.

Zhou, L., Conway, T.J., White, J.W., Mukai, H., Zhang, X., Wen, Y., Li, J. and MacClune, K., (2005). Long-~~ –~~term record of atmospheric CO_2 and stable isotopic ratios at Waliguan Observatory: Background features and possible drivers, 1991–2002. Global Biogeochemical Cycles, **19**(3): GB3021.~~.~~

Formatted: Subscript

Formatted: Subscript

Formatted: Subscript

Formatted: Font: (Default) Times New Roman

Formatted: Font: (Default) Times New Roman

Formatted: Font: (Default) Times New Roman, Subscript

Formatted: Font: (Default) Times New Roman

Formatted: Font: (Default) Times New Roman

Figure 1. Dependence of the observed δ^{13}C on the H_2O mole fraction. The lines represent Equation 2. Error bars are ± one standard deviation. The data in the left panel was obtained on October 1, 2014 using a 439 –µmol mol^{-1}~~ppm~~ standard gas and the true δ^{13}C value of -32.8 ‰, and that in the right panel on June 10, 2015 using a 488 µmol mol^{-1} ~~ppm~~ standard gas and the true δ^{13}C value of -34.1 ‰.

Formatted: Font: Symbol

Formatted: Superscript

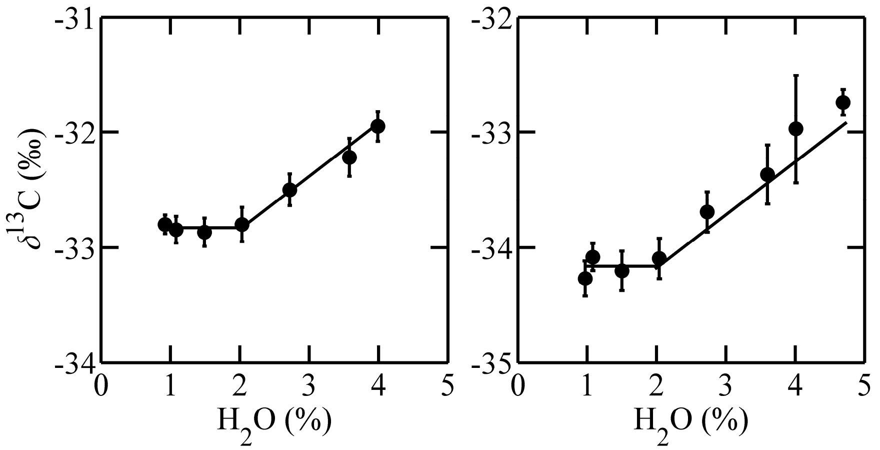

Figure 2. Monthly total CO_2 mole fraction (upper panel) and $\delta^{13}C$ (lower panel): Solid lines with circles: whole-day means; dashed lines with up triangles: daytime (10:00-16:00) means; dashed line with down triangles: nighttime (22:00-6:00) means; smooth solid lines, monthly means observed at WLG.

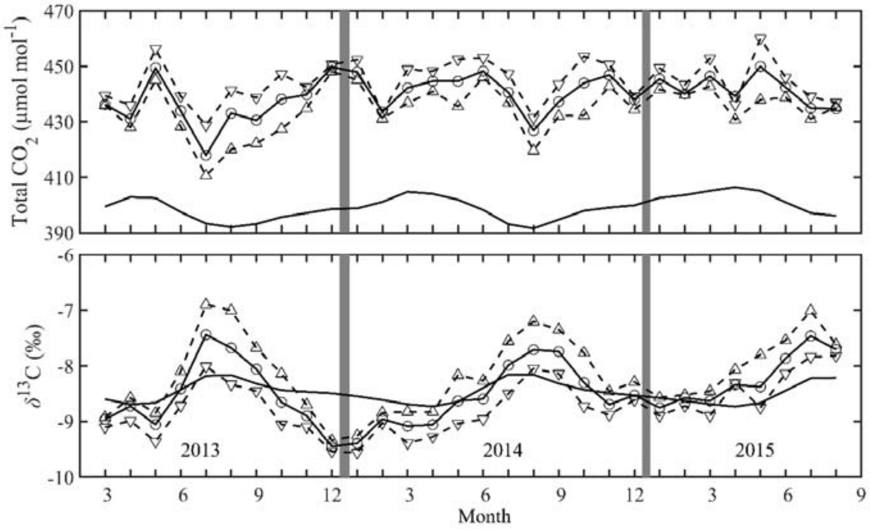

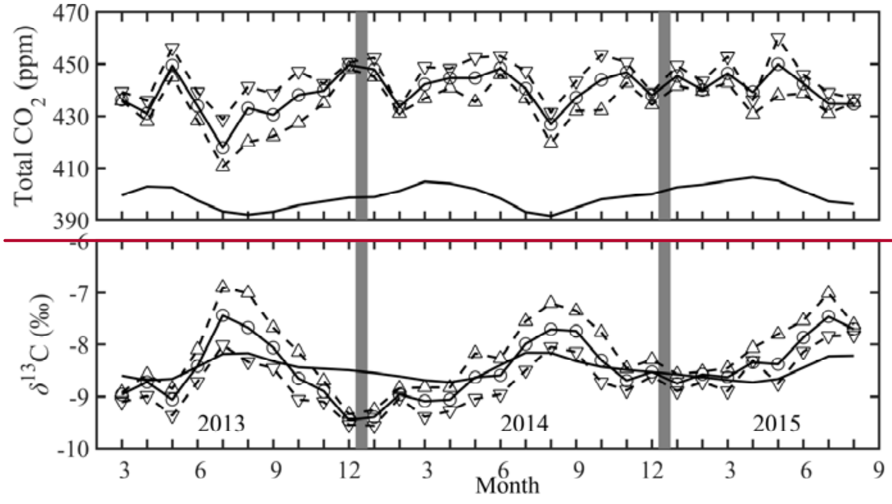

999

Figure 3. Mean die~~urna~~l variation of the CO_2 mole fraction (upper panels) and the $\delta^{13}C$ value (bottom panels) between March, 2013 and August, 2015.

Formatted: Left

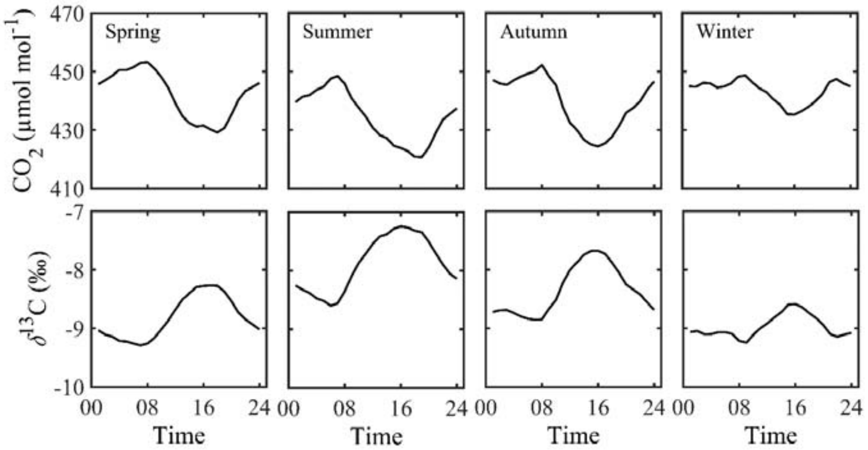

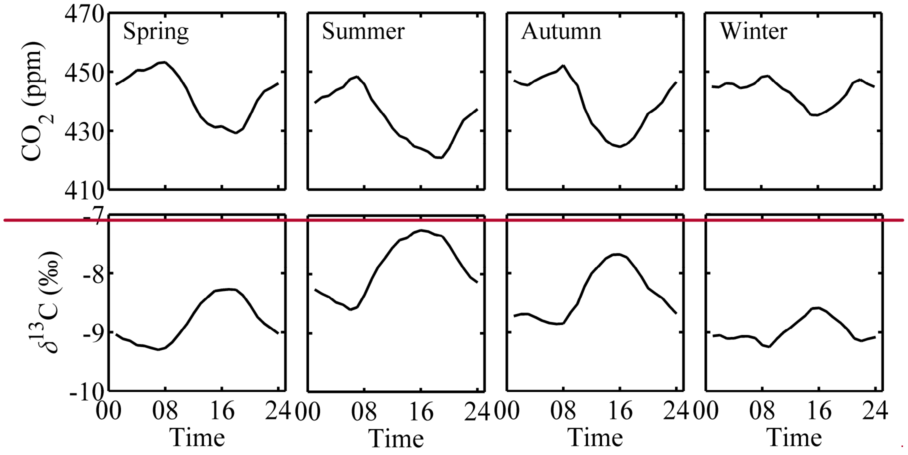

Figure 4. Application of the Miller-Tans method to the~~all valid~~ daytime (10:00-16:00) data obtained in January~~between March, 2013 and August,~~ 2014~~5~~. Each data point is one hourly mean. The solid line is the least squares regression ~~geometric mean regression~~ according to Equation 3~~1~~. Errors bounds on the regression coefficients are 95 % confidence intervals.

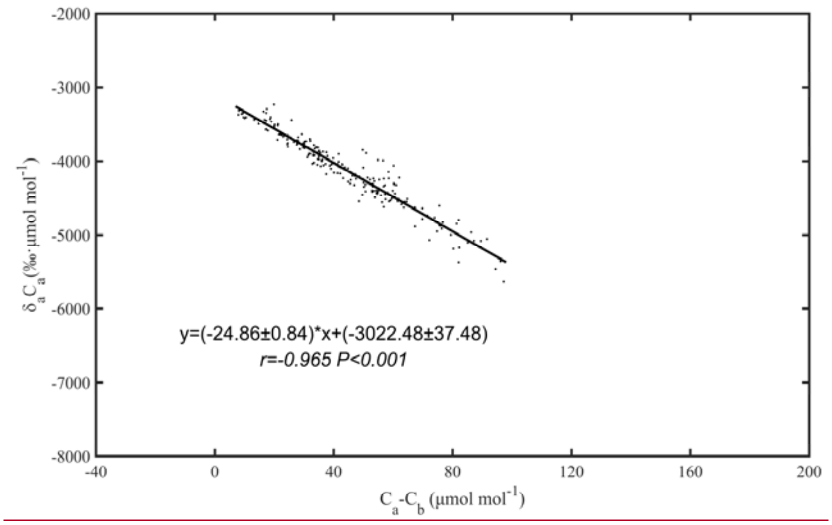

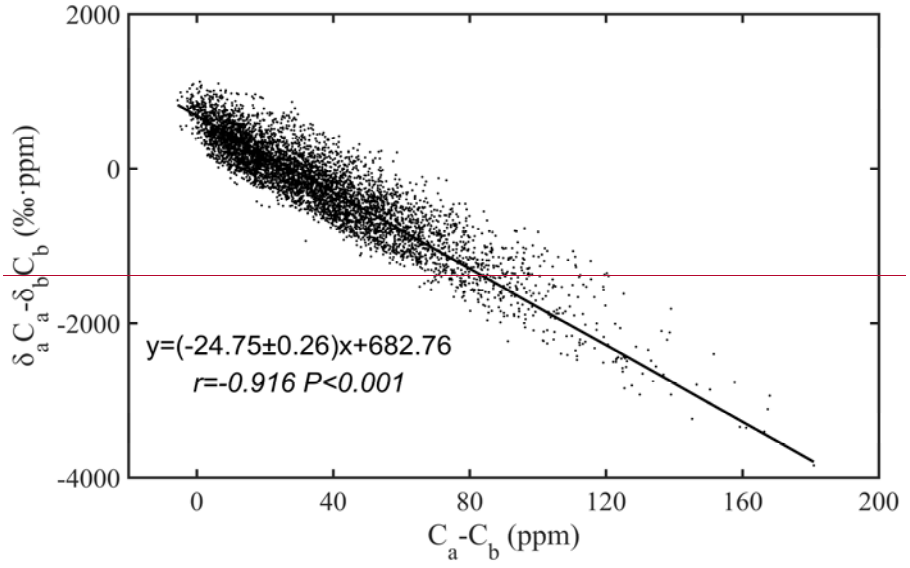

Formatted: Line spacing: Double

Figure 5. Same as Figure 4 but for nighttime (22:00-6:00) data obtained in January 2014.

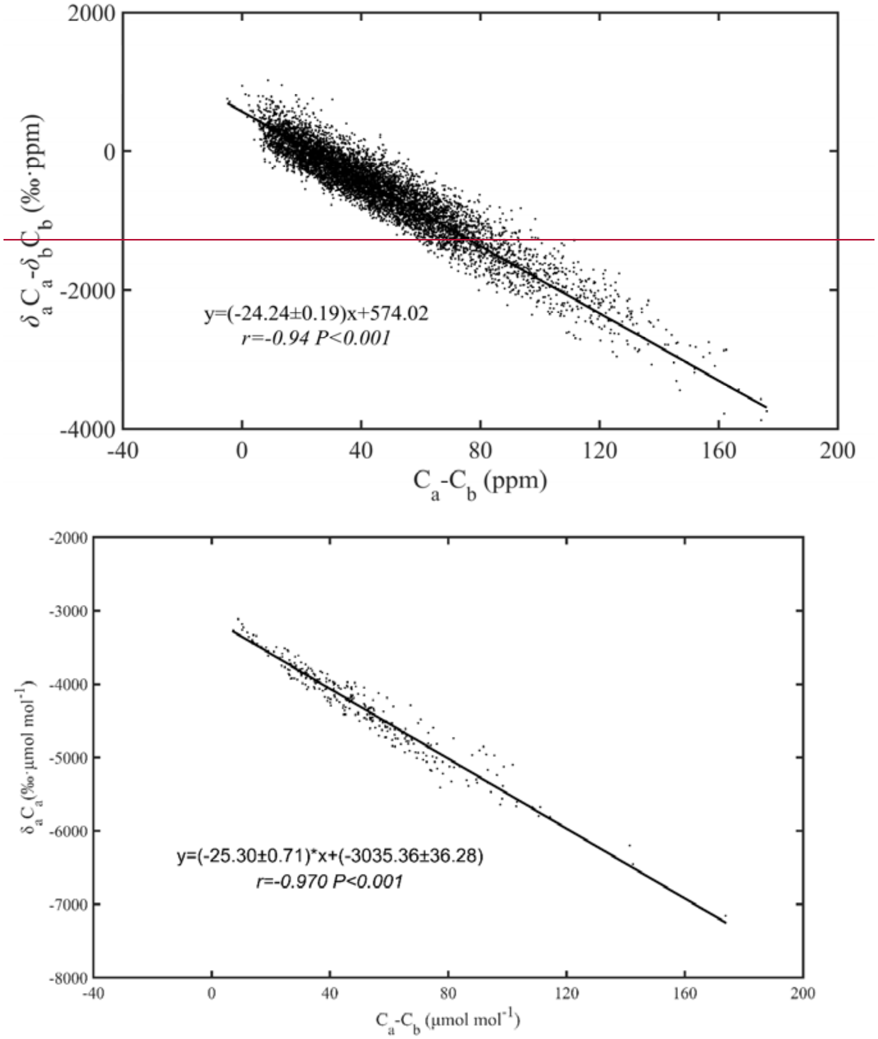

Formatted: Left

Figure 6. Time series of monthly $^{13}C/^{12}C$ ratio~~signature~~ of surface sources in the YRD (a~~black line~~) and in Nanjing (b~~grey line~~), obtained from daytime and nighttime measurement, respectively. The error bars are ± one standard deviation of the~~e Miller-Tans~~ regression coefficient.

Formatted: Superscript

Formatted: Left

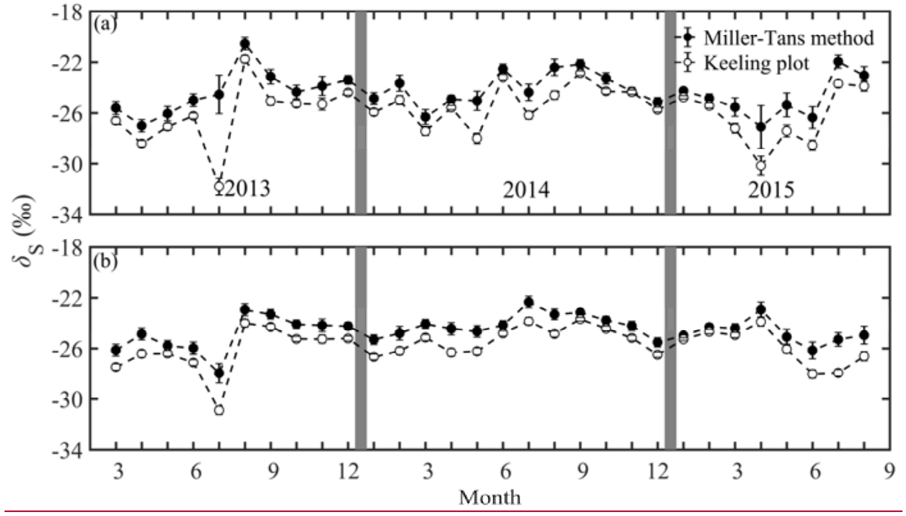

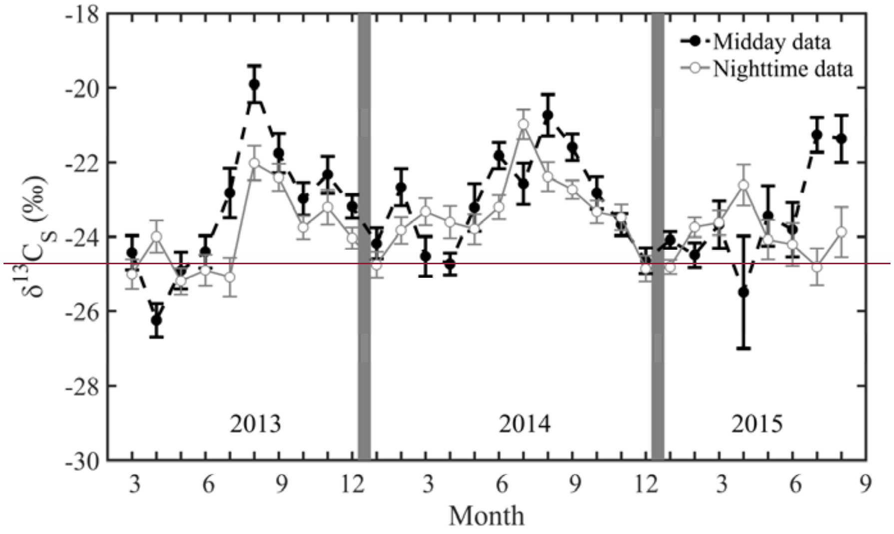

Figure 7. Time series of monthly net surface CO_2 flux (F_S), biological CO_2 flux (F_P), anthropogenic CO_2 flux excluding cement emission (F_F) and cement CO_2 flux (F_c) in the YRD. All the CO_2 mass fluxes are in mg m^{-2} s^{-1}. The flux terms F_F and F_c are assumed to have a 10 % uncertainty typical of fossil fuel consumption data. The partitioning results (F_P and F_S) are based on the source $^{13}C/^{12}C$– ratio~~signature~~ derived from daytime atmospheric measurements.

Formatted: Subscript

Formatted: Subscript

Formatted: Superscript

Formatted: Superscript

Formatted: Left

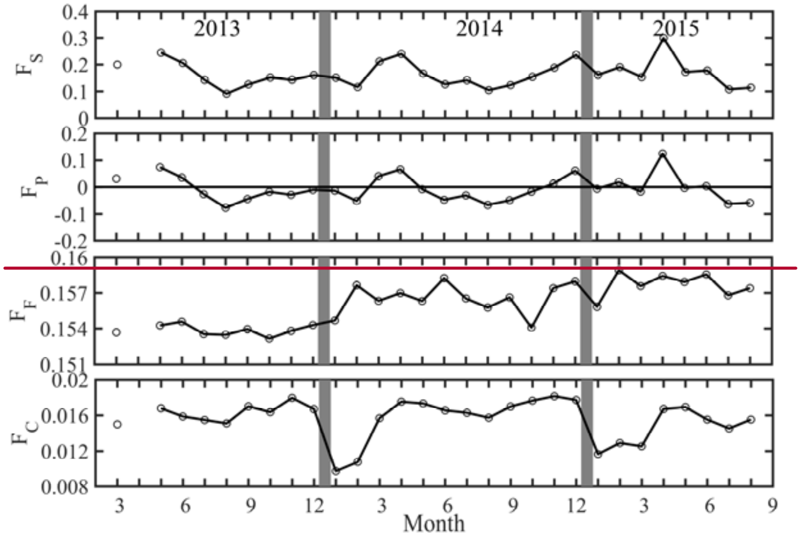

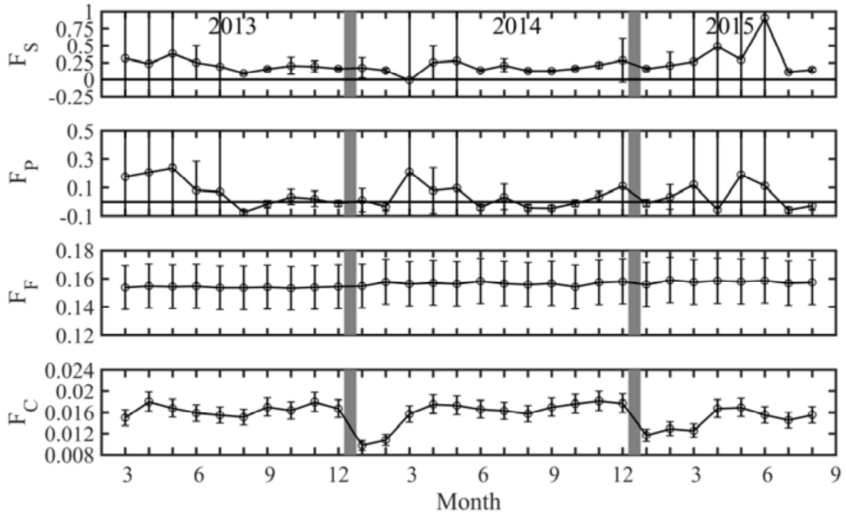
2013
2014
2015
F_S
1
0.75
0.5
0.25
0
-0.25
F_P
0.5
0.3
0.1
-0.1
F_F
0.18
0.16
0.14
0.12
F_C
0.024
0.02
0.016
0.012
0.008
3
6
9
12
3
6
9
12
3
6
9
Month

Figure 8. Time series of monthly net surface CO_2 flux (F_S), biological CO_2 flux (F_P), anthropogenic CO_2 flux excluding cement emission (F_F) and cement CO_2 flux (F_c) in ~~the~~ Nanjing. All the CO_2 mass fluxes are in mg m^{-2} s^{-1}. The flux terms F_F and F_c are assumed to have a 10 % uncertainty typical of fossil fuel consumption data. The partitioning results (F_P and F_S) ~~The results~~ are based on the source $^{13}C/^{12}C$ ratio~~signature~~ derived from nighttime atmospheric measurements.

Formatted: Superscript

Formatted: Superscript

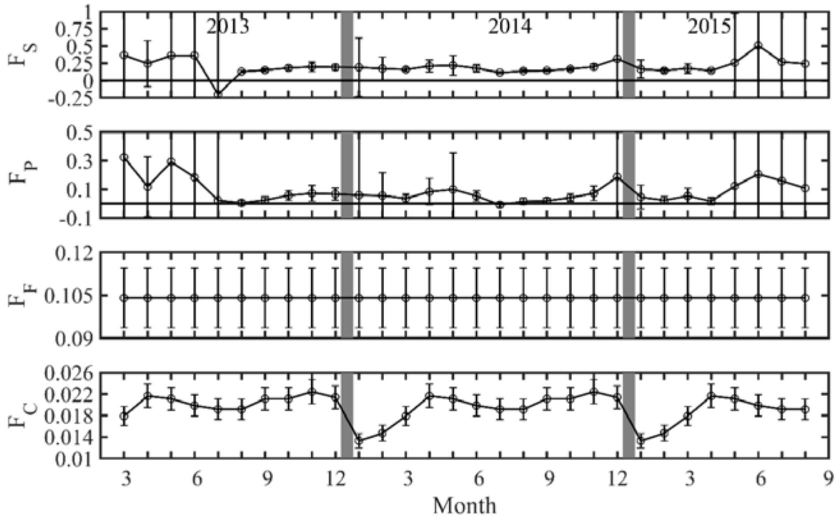
2013
2014
2015
F_S
1
0.75
0.5
0.25
0
-0.25
F_P
0.5
0.3
0.1
-0.1
F_F
0.12
0.105
0.09
F_C
0.026
0.022
0.018
0.014
0.01
3
6
9
12
3
6
9
12
3
6
9
Month

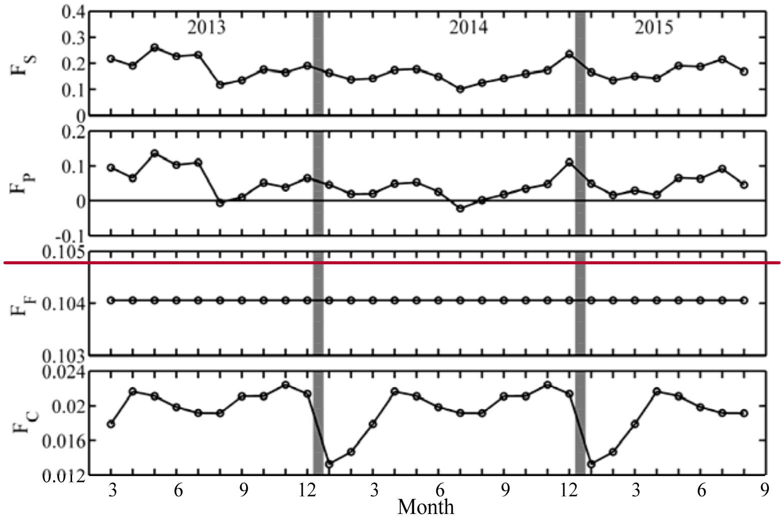
2013
2014
2015
F_S
0.4
0.3
0.2
0.1
0
F_P
0.2
0.1
0
-0.1
F_F
0.105
0.104
0.103
F_C
0.024
0.02
0.016
0.012
3
6
9
12
3
6
9
12
3
6
9
Month

Table 1 Standard gases used for instrument calibration. The mean and standard deviation of the CO$_2$ mole fraction and δ^{13}C were based on 6 and 5 repeated measurements, respectively.

ID	CO$_2$ (µmol mol^{-1}~~ppm~~)	δ^{13}C (‰)	Period
1 Low	381.89 ± 0.99~~381.89~~	-29.75 ± 0.27~~-29.75~~	Mar, 2013 - Aug, 2014
1 High	502.35 ± 0.28~~502.35~~	-30.01 ± 0.18~~-30.01~~	Mar, 2013 - Aug, 2014
2 Low	380.92 ± 0.95~~380.92~~	-29.75 ± 0.27~~-29.75~~	Sep, 2014 - Aug, 2015
2 High	501.05 ± 0.33~~501.05~~	-30.01 ± 0.18~~-30.01~~	Sep, 2014 - Aug, 2015

Formatted: Subscript

Formatted: Font: (Default) Times New Roman, 12 pt

Formatted: Font: (Default) Times New Roman, 12 pt

Formatted: Font: (Default) Times New Roman, 12 pt

Formatted: Font: (Default) Times New Roman, 12 pt

Formatted: Font: (Default) Times New Roman, 12 pt

Formatted: Font: (Default) Times New Roman, 12 pt

Formatted: Font: (Default) Times New Roman, 12 pt

Formatted: Font: (Default) Times New Roman, 12 pt

Formatted: Font: (Default) Times New Roman, 12 pt

Formatted: Font: (Default) Times New Roman, 12 pt

Formatted: Font: (Default) Times New Roman, 12 pt

Formatted: Font: (Default) Times New Roman, 12 pt

Formatted: Font: (Default) Times New Roman, 12 pt

Formatted: Font: (Default) Times New Roman, 12 pt

Formatted: Font: (Default) Times New Roman, 12 pt

Formatted: Font: (Default) Times New Roman, 12 pt

Formatted: Font: (Default) Times New Roman, 12 pt

Formatted: Font: (Default) Times New Roman, 12 pt

Formatted: Font: (Default) Times New Roman, 12 pt

Formatted: Font: (Default) Times New Roman, 12 pt

Formatted: Font: (Default) Times New Roman, 12 pt

Formatted: Font: (Default) Times New Roman, 12 pt

Formatted: Font: (Default) Times New Roman, 12 pt

Formatted: Font: (Default) Times New Roman, 12 pt

Table 2 Percentage of “fossil-plus” sources and their δ^{13}C values for the YRD and Nanjing. The uncertainty in the total “fossil-plus” source is a weighted mean of the individual uncertainties.

	Percentage (%)		δ^{13}C (‰)		
Sources	YRD	Nanjing	YRD	Nanjing	References
Coal	70.0	52.3	-25.46 ± 0.39~~-25.46~~	-25.46 ± 0.39~~-25.46~~	Duan, 1995, Widory 2003~~Duan 1995, Widory 2006~~
Gasoline	2.1	11.4	-28.69 ± 0.50~~-28.80~~	-28.69 ± 0.50~~-28.80~~	Widory and Javoy 2003~~Widory and Javoy 2003~~
Diesel	3.2	1.6	-28.93 ± 0.26~~-29.80~~	-28.93 ± 0.26~~-29.80~~	Widory 2006~~Widory 2006~~
Fuel oil	2.1	0.3	-29.32 ± 0.15~~-28.93~~	-29.32 ± 0.15~~-28.93~~	Widory and Javoy 2003~~Widory and Javoy 2003~~
Natural gas	2.7	5.0	-39.06 ± 1.07~~-39.50~~	-39.06 ± 1.07~~-39.50~~	Widory 2003~~Pang et al. 2016~~
LPG	0.7	0.2	-31.70 ± 0.40~~-31.70~~	-31.70 ± 0.40~~-31.70~~	Widory 2006~~Widory 2006~~
Pig iron	8.7	12.7	-24.90 ± 0.40~~-24.58~~	-24.90 ± 0.40~~-24.58~~	Pan 2007~~this study~~
Crude steel	1.5	0.7	-25.28 ± 0.40~~-24.82~~	-25.28 ± 0.40~~-24.82~~	Wang 2013~~this study~~
Ammonia synthesis	9.0	15.9	-28.18 ± 0.55~~-28.50~~	-28.18 ± 0.55~~-28.50~~	An 2012~~this study~~
Total	100	100	-26.36 ± 0.42~~-26.07~~	-26.9~~4~~7 ± 0.46 ~~2~~	

Formatted Table

Formatted: Font: (Default) Times New Roman

Formatted: Font: (Default) Times New Roman

Formatted: Font: (Default) Times New Roman

Formatted: Font: (Default) Times New Roman

Formatted: Font: (Default) Times New Roman

Formatted: Font: (Default) Times New Roman

Table 3. Inventory data for the isotopic composition of surface CO_2 sources and their percentage of contribution in the YRD and in Nanjing. Here the “fossil-plus” category includes all non-cement anthropogenic emissions listed in Table 2. The cement isotopic ratio is based on Andres et al. (1994). The uncertain range in the biological isotope ratio is based on Vardag et al. (2016).

Sources	YRD		Nanjing	
	δ^{13}C (‰)	Percentage (%)	δ^{13}C (‰)	Percentage (%)
“Fossil-plus”	-26.36 ± 0.42 ~~-26.07~~	91.0	-26.97 ± 0.46 ~~-26.42~~	96.4
Cement	0 ± 0.30 ~~0.20~~	9.0	0 ± 0.30 ~~0.20~~	3.6
Anthropogenic	-23.99 ± 0.41 ~~-23.71~~	100	-26.00 ± 0.45 ~~-25.47~~	100
Biological	-28.20 ± 1.00~~-28.2~~	——	-28.20 ± 1.00~~-28.2~~	——